Assessing the role of terrestrial ecosystems in Finland's total CO$_2$ balance through a comparison of top-down and bottom-up estimates

Kielo Isomäki[1]*, Matthew J. McGrath[2], Leif Backman[1], Juha Leskinen[1], Antoine Berchet[2], Gregoire Broquet[2], Audrey Fortems-Cheiney[2], Virpi Junttila[3], Antti Leppänen[4][1], Hannakaisa Lindqvist[5], Anteneh Mengistu[1], Annikki Mäkelä[6], Maarit Raivonen[4], Laura Thölix[1] and Tuula Aalto[1]

[1] *Climate System Research, Finnish Meteorological Institute, 00560 Helsinki, Finland*
[2] *Laboratoire des Sciences du Climat et de l'Environment (LSCE), CEA CNRS UVSQ UPSACLAY Orme des Merisiers, F-91191 Gif-sur-Yvette, France*
[3] *Finnish Environment Institute (SYKE), 00790 Helsinki, Finland*
[4] *Institute for Atmospheric and Earth System Research, Faculty of Science, University of Helsinki, 00560 Helsinki, Finland*
[5] *Earth Observation Research, Finnish Meteorological Institute, 00560 Helsinki, Finland*
[6] *Institute for Atmospheric and Earth System Research, Faculty of Agriculture and Forestry, University of Helsinki, 00014 Helsinki, Finland*
corresponding author's e-mail: kielo.isomaki@fmi.fi

Large uncertainties persist in quantifying regional CO$_2$ emissions and removals from the land use, land use change, and forestry sector, critical for Finland's climate targets. In support of national greenhouse gas inventories, the scientific community has developed independent top-down and bottom-up approaches to quantify and verify CO$_2$ emissions and removals from biospheric processes. This study merges existing top-down and bottom-up research datasets, including process-based ecosystem models and high-resolution atmospheric inversions, to synthesize available estimates of biospheric CO$_2$ balances from Finnish terrestrial ecosystems. According to the national greenhouse gas inventory, biosphere in Finland removed on average [annual minimum ... maximum] –4.6 [–7.6 … –1.6] Mt C (of CO$_2$) annually between 2012 and 2020. During the same period, regional high-resolution top-down ensemble estimated a mean sink of –12 [–32 … +2.8] Mt C yr^{-1} (deviation pointing to the means of ensemble minimum and maximum) while global top-down ensemble reported a sink closer to inventory with larger deviation between the ensemble members –7.3 [–49 … +32] Mt C yr^{-1}. Corresponding values for regional bottom-up approaches represented by an ensemble of terrestrial ecosystem models closely aligned with the inventory, reporting –4.6 [–21 … +13] Mt C yr^{-1}. The global ecosystem model TRENDY ensemble, with a larger number of ensemble members, estimated an average

---

sink of –9.9 [–30 … +15] Mt C yr^{-1}. Accordingly, we conclude that independent top-down and bottom-up estimates have some consistency in relation to the national greenhouse gas inventory, but at present, large uncertainties found in country-level balances prohibit reliable verification of the inventory.

Introduction

Increasing CO_2 concentration in the atmosphere due to human activities is the main driver of climate change (IPCC 2021). Finland has set an ambitious climate target to become carbon neutral by 2035, balancing production-based CO_2 emissions and removals within its borders (Finnish Government 2022). In 2021, CO_2 fluxes from anthropogenic activities in Finland added about 9.8 Mt C to the atmosphere when including the removals by the biosphere on managed land (CRF 2023). In Finland, land use, land-use change, and forestry sector (LULUCF) has typically acted as a net sink of CO_2. However, over the past decade forest growth rates have declined, while logging activities have intensified causing the LULUCF CO_2 sink capacity to decrease. When considering all GHGs, LULUCF sector transitioned into a net source of emissions in 2021 (NIR 2023). In addition to the reductions of emissions associated with the use of fossil fuels, the emissions and removals from the land use sector hold significant importance to Finland's climate policy, emphasizing the need for timely and precise tracking of emissions and removals from the LULUCF sector.

The reported emissions and removals from LULUCF sector are subject to high uncertainty due to complexity of ecosystems and natural processes as well as limited understanding of ecosystem behavior under varying climatic conditions (e.g., Baldocchi *et al.* 2018, McGlynn *et al.* 2019, Crisp *et al.* 2019). High uncertainty in LULUCF accounting is often not highlighted in the inventory reporting itself, but the uncertainty can undermine the confidence in total reduction claims especially for nations anticipating significant short-term benefits in greenhouse gas reductions from their land-use sectors (McGlynn *et al.*, 2019). In response, the scientific community and key stakeholders are actively working to enhance the accuracy of quantifying carbon sinks and sources within the LULUCF sector and providing methods to verify estimated sources and sinks (e.g. Bastos *et al.* 2022, Deng *et al.* 2022). There are two primary approaches to quantify emissions/removals from land-use sectors: top-down (TD) and bottom-up (BU). These methods have helped to identify potentially underestimated emission sources in inventory accounting (Tenkanen *et al.* 2023) and have exposed knowledge gaps in ecosystem fluxes (Bastos *et al.* 2020). For all that, both BU and TD approaches too are prone to large uncertainties and discrepancies continuing to persist both between and within methodological approaches (e.g. Grassi *et al.* 2022, Grassi *et al.* 2018). Nonetheless, particularly TD approaches are evolving rapidly due to advancements in computational and observation methods, like higher resolution and increasing coverage of satellite observations, resulting in reduced uncertainties (e.g., McGrath *et al.* 2023, Bastos *et al.* 2022).

Rapid progress highlights the importance of analyzing the newest available data together with its uncertainty ranges, and of monitoring how advancements in observation-based methods affect the estimated total carbon balances. Further, understanding of the discrepancies between the approaches continuously improves (e.g., Ciais *et al.* 2022; Munassar *et al.*, 2023) which allows more reliable comparison of the different estimates. This paper contributes to the previous literature by consolidating existing research datasets and assessing their CO_2 flux estimations and delineating ranges of uncertainty at the national level enabling the consideration of local issues. Many previous studies have instead been carried out at the regional scale, which permits a less-detailed analysis given methodological differences between inventories from country to country (e.g. Petrescu *et al.* 2021). Other GHGs than CO_2 are excluded from the analysis. By contrasting these research datasets with Finland's national inventory and spatially explicit forest growth model PREBAS, the study further contributes to the discourse on the application

of atmospheric observations to validate regional carbon balances.

Finland's climate policy framework is guided by international climate agreements like the United Nations Framework Convention on Climate Change (UNFCCC), Paris Agreement (Paris Agreement 2015) and EU's climate and energy politics (EU 2021). Being part of the Annex-1 countries in the UNFCCC, Finland must provide information on its anthropogenic greenhouse gas emissions and removals annually in the form of a national greenhouse gas inventory (NGHGI). Finland's NGHGI estimates annual emissions and removals using a bottom-up approach that quantifies emissions based on activity data and emission factors while the sinks (i.e. removals of CO_2) are driven from inventories of carbon stock changes and models following 2006 Intergovernmental Panel on Climate Change (IPCC) guidelines (IPCC 2006).

NGHGIs classifies emissions and removals in five sectors: 1) energy; 2) industrial processes and product use; 3) agriculture, 4) LULUCF; and 5) waste. When the activity data and emission factors are well known, inventories can provide accurate national estimates of the actual emissions for categories such as fossil fuel combustion. In the LULUCF sector, significant uncertainties in emission factors and models arise from structural and conceptual challenges. These include considerable heterogeneity of fluxes across time and space, influenced by both natural and anthropogenic processes, the lack of continuous data over time and large areas, and the differences in methods and definitions (McGlynn *et al.* 2019).

In support of NGHGIs, independent research groups and institutions provide a range of CO_2 emission and removal estimates. Both BU and TD approaches are commonly used to quantify both anthropogenic and natural carbon sources and sinks at global, regional, and national level (e.g., Friedlingstein *et al.* 2022). The former approach implies the assessment of carbon fluxes for individual processes contributing to the global carbon cycle by applying observed activity data, empirically collected emission factors, and modeling techniques (e.g. quantities and types of combusted fossil fuels, changes in leaf area index or land use through satellite

observations) (NIR 2023, Bastos *et al.* 2023). BU approaches include a variety of methods from physical ecosystem models to data-driven bookkeeping and categorical models like the NGHGIs. Concerning bottom-up approaches, this paper focuses specifically on terrestrial ecosystem models that simulate vegetation productivity and carbon cycling under changing climatic conditions based on mathematical descriptions of ecosystem behavior (Piao *et al.*, 2013).

In contrast to BU methods, TD approaches employ atmospheric observations of CO_2 concentrations coupled with atmospheric transport models to assimilate spatially explicit and globally consistent exchange of carbon between the land surface, ocean, and the atmosphere (e.g., Bastos *et al.* 2020). The atmospheric observations of varying CO_2 concentrations reflect the state of the global carbon cycle, encompassing emissions from human activities and natural sources, as well as absorption of carbon by terrestrial biosphere and oceans (Chevallier 2021.). While inventory and BU approaches provide essential data about the development of anthropogenic emissions and establish the basis of emission reduction scenarios and policy frameworks, complementary TD approaches offer an independent perspective to the carbon cycle. TD approaches are consistent with the global growth rate of CO_2 concentrations unlike the BU methods. Recent advancements in top-down approaches, including an increased number of atmospheric observations and higher model resolution, have allowed the extraction of data for smaller regions and even individual countries with the first high-resolution country-level results considering CO_2 fluxes being published in the early 2020s (McGrath *et al.* 2023, Petrescu *et al.* 2021, Byrne *et al.* 2023).

The IPCC guidelines encourage countries to verify emissions and removals reported in NGHGIs through independent data sources (IPCC 2019). However, achieving comparability between different approaches is challenging as it involves reconciling discrepancies in the fluxes each approach accounts for, and harmonizing definitions among scientific community and national inventory agencies (Bastos *et al.* 2022). In addition to the divergence in definitions, discrepancies in the estimates arise from differences

in model structures and underlying datasets. During the last couple of years, the scientific community has made an effort towards reconciling country specific NGHGIs with global and regional TD and BU datasets (e.g. Grassi *et al.*, 2022; Deng *et al.*, 2022; Chevallier *et al.*, 2021; Grassi *et al.*, 2018). However, more efforts are needed to understand the application of these regionally harmonized approaches at the country level which could increase the confidence to utilize the global/regional datasets, e.g., by national inventory agencies (using the methods recommended by the IPCC). For example, the accuracy of inversion fluxes may differ depending on factors such as the size of the country, which can be problematic for small countries if the resolution of the inversion is coarse. In addition, the density of in-situ observation network or the conditions under which satellites take measurements over the country also influence the accuracy of TD estimates (Bastos *et al.*, 2022). Due to its relatively large size and high number of in-situ observation stations, Finland is an interesting case study for analyzing the national budgets derived from atmospheric observations.

All approaches and individual models included in this study provide an estimate of the net CO_2 flux between the land surface and the atmosphere. This comprises carbon uptake through photosynthesis and emissions caused by respiration and disturbances. However, comparing CO_2 balances between multiple approaches requires understanding of the component fluxes included in the estimate, as some approaches might report the "total" exchange and the others a "partial" exchange of CO_2 (Kondo et al 2020). For example, atmospheric inversions report the total exchange whereas the NGHGIs account only for managed land to capture the anthropogenic emissions (Chevallier 2021, NIR 2023).

In Finland, forest ecosystems sequestrate significant amounts of CO_2, and soon Finland expects the LULUCF sector to offset all GHG emissions from other sectors. At the same time, forestry is one of the main economic sectors in Finland (Ministry of Agriculture and Forestry 2023), and with increased loggings and reduced tree growth, CO_2 removals on forest land in Finland have declined during the last decade (Haakana *et al.* 2022). Identifying economically

sustainable forest management strategies that support climate change mitigation has become a key challenge (Junttila *et al.* 2023, Forsius *et al.* 2023). Different land carbon and forest growth models are used to study emission pathways under various management and climate scenarios (Junttila *et al.*, 2023) but these models often lack validation of the country-level carbon balances. Evaluation of these models with accurate and consistent observation-based estimates of the terrestrial carbon balances, e.g., from atmospheric inversions, could contribute to increasing reliability of the resulting emissions pathway scenarios (Ciais *et al.* 2022).

This article provides an evaluation of a forest growth model PREBAS against the newest regional atmospheric inversions over Finland. PREBAS (Valentine and Mäkelä 2005, Peltoniemi *et al.* 2015, Minunno *et al.* 2019) is a process model designed to investigate the influence of various forest management strategies on carbon pools within Finnish forest ecosystems (Junttila *et al.*, 2023). PREBAS provides a good basis for the evaluation since it operates on extremely high spatial resolution. It combines field-based inventory and remote sensing data providing a detailed description of forest structure throughout Finland which is similar to the Finnish national inventory. In Finland, forest ecosystems are the primary contributors to biospheric CO_2 fluxes which implies that a significant proportion of the inversion fluxes should come from the most forested areas. Thus, such comparison can provide additional information about the representativeness of atmospheric inversions in Finland. Note that in this study, we will only consider the base scenario (Junttila *et al.* 2023), and no results related to forestry management scenarios are presented.

This paper aims to thoroughly evaluate the Finnish carbon balance estimates from a broad range of the up-to-date research datasets. The paper will first demonstrate the total balance derived from TD and NGHGI methods after which biospheric and forest-specific aspects are discussed in more detail. By integrating global and regional findings into a national context, we intend to map out available results and compile them comprehensively. This will result in a more profound understanding of available biospheric

flux estimates and their representativeness in Finland. This paper will achieve the objectives by: 1) synthesizing existing research datasets, and comparing them with Finland's greenhouse gas inventory; 2) examining how climatic conditions impact both bottom-up and top-down estimates; 3) comparing forest growth model (PREBAS) and atmospheric observations interpreted by regional high-resolution atmospheric inversions; and 4) discussing methodological differences and uncertainty estimates between the BU and TD approaches.

Material and methods

National Greenhouse Gas Inventory of Finland

The annual greenhouse gas inventory includes information on the country-level emissions and removals since 1990, the latest 2023 inventory covering years until 2021 (CRF 2023). The methods that can be applied in NGHGI are specified in the 2006 IPCC Guidelines for National GHG Inventories (NIR 2023). This paper presents the removals and emissions of the LULUCF sector, and emissions from other sectors estimated in the 2023 inventory report.

LULUCF sector constitutes the following land use categories: Forest land, Crop land, Grass land, Wetlands, Settlement, and Other land. In addition, inventory accounts for changes from one land use category to another. Estimates of emissions and removals in the LULUCF sector are based on inventories of carbon stock changes in different pools on an annual time step. Country specific methods to estimate these changes in Finland include, e.g., a forest inventory conducted every five years by LUKE (Korhonen *et al.* 2021), and process models, such as Yasso07 for soil carbon stock changes (Liski *et al.*, 2005). Besides the removals and emissions from the land use categories, LULUCF sector considers the carbon stock changes in Harvested wood products (HWP).

In the context of Finland, the predominant sink of CO_2 occurs within Forest land due to biomass growth followed by transfer of carbon to the HWP pool, whereas all other land use categories contribute to CO_2 emissions (NIR, 2023). Within Forest land, various carbon pools are considered, including living biomass, dead wood, litter, and soil organic carbon. The most important components of the CO_2 balance within Forest land are tree biomass growth (derived from the forest inventory) and the removal of biomass through logging activities, which together yield the annual living biomass stock change. Carbon loss from disturbances, such as windthrow and bark beetles, is reflected in the forest inventory and thereby those are not considered separately. Emissions caused by utilization of wood, e.g., in energy production, are accounted for as emissions within the LULUCF sector. However, when harvested wood is transformed into timber products, it remains as a carbon sink in the HWP category, having a small half-life coefficient. (NIR, 2023). The carbon stock changes in the Forest land are assessed through forest inventory every five years, which balances out some of the year-to-year fluctuations in the total balance due to interannual variations in weather patterns and logging activity.

In the LULUCF inventory, dead wood, litter and soil organic matter are reported in a combined pool for both organic and mineral soils. Dead wood is a pool that originates from natural mortality of the trees and from residual wood waste due to logging. Litter is a carbon pool that includes both above-ground and below-ground litter. The litter input to the soil is estimated based on the biomass of vegetation (other than trees), dead foliage, leaves, branches, roots etc. Carbon stock in soil organic matter is built up by the decomposed litter accumulated in soils. The soil carbon model Yasso07 (Liski *et al.*, 2005) estimates the total carbon stock in soil and its changes. Similar methods to compute soil organic carbon are often used in other bottom-up models.

The purpose of NGHGIs is to estimate and report anthropogenic emissions, and thus the NGHGI does not cover the total carbon balance of Finland but aims to capture the human induced changes. In the LULUCF sector the distinction between anthropogenic and natural emissions and/or removals is not clear due to indirect effects of, e.g., increasing CO_2 levels (Grassi *et al.* 2022, Chevallier 2021). The IPCC

has suggested using "managed land" as a proxy for anthropogenic emissions and removals. This means that all emissions and removals from managed land are accounted for in the inventory. Managed land is defined as "land where human interventions and practices have been applied to perform production, ecological or social functions" (IPCC 2019, p. 806). In Finland "managed land" covers about 80% of total area excluding e.g. emissions and removals from undrained wetlands and conservation areas.

The accuracy of methods applied in inventory varies from Tier 1 to 3. Tiers 1 and 2 multiply activity data with emissions factors that are country specific in Tier 2 and global averages in tier 1. Tier 3 methods are considered to yield more accurate results and in the LULUCF sector, and Tier 3 methods include e.g., country-specific models, or repeated field measurements (McGlynn *et al.* 2018, NIR 2023). The uncertainty of the total LULUCF sector for Finland was taken from data products provided by McGrath *et al.* (2023) as the inventory reporting does not provide aggregated uncertainty for total LULUCF or individual GHGs. We converted CO_2-equivalent emissions and removals reported in the NGHGI to carbon by multiplying them by 12/44.

CO_2 flux research datasets

Net Biome Production

We defined Net Biome Production (NBP) as the total or partial exchange of carbon between the terrestrial biosphere and the atmosphere. NBP (Eq. 1) denotes the net production of organic matter in a region through photosynthesis. It composes the loss of organic matter due to plant and soil respiration (R_{eco}), and through other natural and anthropogenic disturbances (*D*). Depending on the approach, the inclusion of natural (e.g. forest growth, climate-variability-induced carbon fluxes, forest fires) and anthropogenic processes (e.g. deforestation, harvest) contributing to photosynthetic processes and disturbances can vary as described later. The sign convention follows the principle that a negative value for NBP represents a flux from the atmos-

phere to the land, i.e., a carbon sink within the biosphere.

$$NBP = D + R_{eco} - GPP \qquad (1)$$

Terrestrial Ecosystem Models

Dynamic Global Vegetation Models

Concerning bottom-up methods, this paper has emphasis on the CO_2 flux estimates of terrestrial ecosystem models that can be used to assess the global spatio-temporal dynamics of land-atmosphere fluxes. This paper comprised five independent runs of Dynamic Global Vegetation Models (DGVM), one global DGVM ensemble (TRENDY-v11, Friedlingstein *et al.* 2022), and one forest growth model specific to Finnish conditions (PREBAS, Junttila *et al.* 2023) as outlined in Table 1. Terrestrial ecosystem models, such as the DGVMs, derive the biospheric CO_2 fluxes from mathematical representations of biochemical, ecological, and physical processes responsible for these fluxes. Such processes comprise e.g. the hydrological cycle, solar radiation's influence on photosynthesis, and nutrient cycling. Terrestrial ecosystem models contribute to comprehensive modeling of terrestrial carbon cycle by quantifying carbon pools on land surface and their dynamical behavior in response to either static or changing climatic conditions. Drivers for those models are air temperature, wind speed, solar radiation, air humidity, precipitation, and atmospheric CO_2 concentrations. These drivers together with the state of land surface regulate the fluxes of carbon, water, energy, and momentum in each simulated grid cell. The state of the land surface is determined by regional vegetation systems and their structural attributes that vary based on local climate. Specific to DGVMs, vegetation is defined with several vegetation types that are called plant functional types (Woodward & Wolfgang 1996).

From the beginning of a DGVM simulation, the vegetation starts to grow which cycles the carbon between atmosphere, biosphere and soil through photosynthetic processes. One of the primary outputs of DGVMs is the bottom-up NBP that is the sum of gross primary production (GPP), ecosystem respiration and CO_2

Table 1. Description of data.

Dataset/Model name	Provider	Period covered, resolution	Variables	Reference
Anthropogenic CO$_2$ fluxes				
Inventory				
National Greenhouse Gas Inventory (2023)	Statistics Finland	1990–2021, Country total	CO$_2$ emissions from Energy, Industrial Processes and Product Use, Agriculture, and Waste sectors	NIR (2023) CRF (2023)
EDGAR-v4.3 EDGAR/TNO	VERIFY	2006–2021 0.5° × 0.5°	Prior anthropogenic emissions of V2021 inversions. Emissions are based on British Petroleum statistics and distributed spatially and temporally with COFFEE approach.	McGrath *et al.* (2023, see Appendix A2) COFFEE approach (Steinbach *et al.* 2011)
Land CO$_2$ Fluxes				
Inventory				
National Greenhouse Gas Inventory (2023)	Statistics Finland	1990–2021, Country total	LULUCF CO$_2$ emissions and removals	NIR (2023) CRF (2023)
Terrestrial Ecosystem Models				
ORCHIDEE (for V2021)	LSCE	1990–2021, 0.125°x 0.125°	Bottom-up CO$_2$ fluxes from plant uptake; soil decomposition; and harvests across forests, grasslands, and croplands	Ducoudré *et al.* (1993) Viovy (1996) Polcher *et al.* (1998) Krinner *et al.* (2005) McGrath *et al.* (2023)
LPX-BERN (for V2021)	University of Bern	1990–2021, 0.125°x 0.125°	Bottom-up CO$_2$ fluxes from plant uptake; soil decomposition; and harvests across forests, grasslands, and croplands	Lienert and Joos (2018)
CABLE-POP (for V2021)	Western Sydney University	1990–2021, 0.125°x 0.125°	Bottom-up CO$_2$ fluxes from plant uptake; soil decomposition; and harvests across forests, grasslands, and croplands	Haverd *et al.* (2018) McGrath *et al.* (2023)
JSBACH	FMI UH INAR	2017–2021, 1°x 1°	Bottom-up CO$_2$ fluxes from plant uptake; soil decomposition; and harvests across forests, grasslands, and croplands	Reick *et al.* (2021)
LPJ-Guess	FMI	1900–2021, 0.5°x 0.5°	Bottom-up CO$_2$ fluxes from plant uptake; soil decomposition; and harvests across forests, grasslands, and croplands	Smith *et al.* (2001) Smith *et al.* (2014)

Table 1. (*continued...*)

Dataset/Model name	Provider	Period covered, resolution	Variables	Reference
Land CO_2 Fluxes				
Terrestrial Ecosystem Models				
PREBAS	Helsinkik UNI	Annual mean of 2017–2025, 16 m × 16 m	Annual mean Net Ecosystem Exchange (NEE) & NBP = NEE – harvest	Valentine & Mäkelä (2005) Minunno *et al.* (2016) Minunno *et al.* (2019)
TRENDY v11 (inc. 15 models following identical simulation protocols, S3 TRENDY protocol)	MetOffice UK	1900–2020, 0.125° × 0.125°	Bottom-up CO_2 fluxes from plant uptake; soil decomposition; and harvests across forests, grasslands, and croplands	Friedlingstein *et al.* (2022; see Table 4 for detailed references)
Regional (high resolution) Atmospheric Inversions				
CarboScopeRegional, CSR (for V2021, inc. 4 simulations)	MPI-Jena	2006–2021, 0.25° × 0.25°	Total inverse CO_2 flux from terrestrial ecosystems (NBP)	Kountouris *et al.* (2018) Munassar *et al.*, (2022) Munassar *et al.*, (2023)
LUMIA (for V2021, inc. 3 simulations)	Lund University	2006–2021, 0.5° × 0.5°	Total inverse CO_2 flux from terrestrial ecosystems (NBP)	Monteil and Scholze (2021) McGrath *et al.* (2023)
CIF-CHIMERE (for V2021)	LSCE	2005–2020, 0.5° × 0.5°	Inverse CO_2 flux from terrestrial ecosystems (NBP)	Berchet *et al.* (2021) Broque *et al.* (2013)
EUROCOM 2019 (inc. 6 models: CSR, LUMIA, CHIMERE, FLEXINVERT, CTE, EnKF-RAMS)		2006–2015, Varying resolutions	Inverse CO_2 flux from terrestrial ecosystems (NBP)	Monteil *et al.* (2020) Petrescue *et al.* (2021)
Global Atmospheric Inversions				
v10 OCO-2 MIP IS, LNLG and LNLGIS experiments (inc. 14 models run with standard protocol: AMES, Baker, CAMS, CMS-Flux, COLA, CSU, CT, JHU, LoFI, NIES, OU, TM5-4DVar, UT, WOMBAT)	GML	2015–2020, Simulations run with variety of resolutions, but final data product re-gridded to 1° × 1°	Inverse CO_2 flux from terrestrial ecosystems (NBE ~ NBP). *IS* is assimilated with in situ measurements, *LNLG* assimilates ACOS v10 land nadir and land glint total column dry-air mole fractions retrieved from OCO-2 satellite. *LNLGIS* assimilates in situ and satellite retrievals over land together	Byrne *et al.* (2023; see Table 1 for detailed references)

Table 1. (*continued...*)

Dataset/Model name	Provider	Period covered, resolution	Variables	Reference
Land CO_2 Fluxes				
Global Atmospheric Inversions				
GCB 2021 (inc. 6 models: CTE, CAMS, CarboScope, NISMON-CO2, UoE, CMS-Flux)	GCP	2010–2020, Varying resolutions	Total CO_2 inverse flux from terrestrial ecosystems (NBP)	Friedlingstein *et al.* (2022; see Table 4 for detailed references)
CarbonTracker (CT)	FMI	2017–2021, 1° × 1° over Europe, coarser elsewhere	Total CO_2 inverse flux from terrestrial ecosystems (NBP)	van der Laan-Luijkx *et al.* (2017) Prior fluxes used here: Biospheric: JSBACH Anthropogenic: EDGARv6, Ocean: Van der Woude *et al.* (2023)

fluxes associated with disturbances on a gridded domain (similar to Eq. 1). The models, however, simulate bottom-up NBP with varying numbers of ecosystem carbon pools and fluxes. Part of the natural vegetation systems are disturbances caused by natural hazards e.g. fires and droughts, but the representation of disturbances differs from model to model. Most of the existing DGVMs also account for anthropogenic disturbances, such as land use transitions and forest and crop harvests. The latter two are usually described as bulk removals of biomass each year. The land use transitions, however, are derived from land use maps that are often collected with remote sensing data but can additionally contain information about national harvest data.

PREBAS

PREBAS is a combination of forest growth (Valentine and Mäkelä, 2005) and forest gas flow models (Peltoniemi 2015). It differs from the DGVMs by assimilating CO_2 fluxes from Finnish forest ecosystems only (croplands, for example, are not included), and it applies real forest structure data, and realistic management scenarios derived from Finnish recommendations (Mäkelä *et al.* 2023), with model parameters specific to Finland. PREBAS is a process-based model that computes carbon sequestration through an explicit

description of photosynthesis. PREBAS allocates the resulting GPP to respiration and mean-tree-growth at an annual time step. PREBAS is driven by inputs of radiation, temperature, vapor pressure deficit, precipitation, and ambient CO_2 concentration (Peltoniemi *et al.* 2015, Minunno *et al.* 2016, Kalliokoski *et al.* 2018). The PREBAS fluxes have been calibrated using eddy covariance data from Fennoscandia, and the growth model has been calibrated based on growth experiments in Finland (Minunno *et al.*, 2016). To derive the complete net ecosystem exchange (NEE, Eq. 2) of forests, a ground vegetation module based on ground vegetation inventories (Tonteri *et al.* 2005,) and soil carbon processes based on the Yasso07 (Liski *et al.* 2005) model have been integrated into PREBAS.

$$NEE = R_{eco} - GPP \qquad (2)$$

For this study, the output of PREBAS model was nine years' annual average gridded (16 m × 16 m) NEE. The simulation was done using the current climatic conditions and base harvest scenario that corresponds to the current harvest levels in Finland (Junttila *et al.* 2023). Based on the model output NEE, the CO_2 balance (NBP) of the forest ecosystems was obtained as the sum of NEE (negative NEE indicates a sink) and harvested biomass (Junttila *et al.* 2023). To compare PREBAS output with all other approaches, both

NEE and NBP were computed. For this paper, the output of PREBAS was interpolated to a coarser resolution to match the atmospheric inversions.

Top-Down

This paper demonstrates the total and biospheric carbon balance of Finland as seen by four individual high resolution atmospheric inversions (CSR, LUMIA, CIF-CHIMERE, CT) (Table 1) of which CSR, LUMIA, and CIF-CHIMERE simulations were available through EU-H2020 VERIFY project (V2021) and published by McGrath *et al.* (2023). The biospheric estimates of these TD datasets are contrasted against previously published global and regional inversions ensembles including EUROCOM (Monteil *et al.* 2020, Petrescu *et al.* 2021), and Global Carbon Budget (GCB) (Friedlingstein *et al.* 2022). We also included newly published v10 Orbiting Carbon Observatory (OCO-2) modeling intercomparison project (MIP) global inversion ensemble utilizing satellite measurements (Byrne *et al.* 2023). V10 OCO-2 MIP data were downloaded from [https://gml.noaa.gov/ccgg/OCO2_v10mip], last accessed: [12 August 2023].

Top-down approaches, essentially atmospheric inversion, provide observation-based estimates of the total land-atmosphere CO_2 fluxes. Atmospheric inversions are given the prior value of CO_2 sinks and sources, the CO_2 observations from atmospheric measurements (in-situ and/or satellite), and uncertainty distributions for both. The inversion then optimizes the difference between the observed and prior information allocating the quantities of CO_2 emissions and removals to the most probable locations based on atmospheric transport and statistical approaches. The prior information of biospheric fluxes can be either DGVM output, inventory data or a product of both with associated uncertainties. Inversions usually assimilate the optimal CO_2 flux as a maximum likelihood estimate following Bayesian statistical approach (Rodger 2000). The number of available atmospheric observations influences the independence of assimilated inversion fluxes.

Atmospheric inversions account for the effect of fossil fuel and cement production CO_2 emissions on the concentration gradients by giving the transport model a fixed map of the assumed fossil CO_2 emissions. Because of the small uncertainty associated with fossil fuel emissions, many of the TD approaches utilize prescribed information on fossil fuels without optimization. The prior signal of fossil emissions is removed in the pre- or post-processing of the inversion outputs which over land area yields the non-fossil CO_2 fluxes. Non-fossil CO_2 fluxes assimilated by the inversion methods include gross primary production, plant and soil respiration, litter photo-oxidation, biomass burning (both wildfires and biomass combustion in energy production), inland water fluxes etc. Inversions do not have the ability to attribute fluxes into these subcategories and inversions generally report the CO_2 fluxes in four categories: fossil, land, ocean, and fire fluxes. In addition to fossil fuel fluxes, ocean and fire fluxes are generally prescribed, and therefore land fluxes (total CO_2 flux from terrestrial ecosystems ~ NBP) include all remaining fluxes.

Lateral carbon fluxes

Atmospheric inversions consist of all components of the carbon cycle that compose the CO_2 gradients between measurement stations. In other words, inversion fluxes are the total land-atmosphere CO_2 fluxes at any given location, meaning that the inversion cannot distinguish between carbon uptaken through photosynthesis and that emitted through respiration. Thus, the impact of lateral transport of carbon is implicitly included in the optimized fluxes (Ciais *et al.* 2006). This is different compared with bottom-up methods, that employ production-based accounting which reports the removals and emissions from activities like wood harvesting at the explicit locations that they occur (ecosystem models on grid-level, and inventories on country-level). Therefore, when carbon is absorbed by vegetation in a particular region and subsequently emitted elsewhere, bottom-up and top-down approaches record this differently.

To facilitate comparison between BU and TD balances, TD fluxes are adjusted with lateral fluxes of carbon that are carbon fluxes resulting from international crop and wood trade together with transportation of carbon through inland

water networks. Lateral carbon fluxes can be estimated by combining international trade data (imported and exported wood and crop commodities) together with estimates of the biospheric CO$_2$ uptake that is leached into inland waters (Ciais *et al.* 2022). The imports and exports of traded wood and crop commodities are classified as either carbon sources or sinks: domestically produced commodities act as carbon sinks, whereas the carbon source is defined as the sum of domestic production and imports, reduced by exports. Given that the positive inversion flux value is a flux into the atmosphere, the lateral flux caused by the crop and wood trade is the sum of sink (denoted by a negative value) and source (denoted by a positive value) components. Consequently, the adjustment of inversion fluxes decreases the country level sink if nation's exports of wood and crop commodities surpass the imports and vice versa. In the case of inland water sinks and sources, the CO$_2$ uptake that is leached into the inland water network within the country borders represent the CO$_2$ sink, and the source constitutes of the carbon that is released back to the atmosphere from the dissolved CO$_2$ or breakdown of other organic matter.

We adjusted the total annual inversion budgets with the lateral fluxes prepared by McGrath *et al.* (2023) following Deng *et al.* (2022) and Ciais *et al.* (2021). Lateral fluxes associated with international trade were obtained from FAO national wood and crop trade statistics where production, import and export of each commodity were aggregated to country-level and converted to carbon with suitable conversion factors (McGrath *et al.*, 2023). The lateral fluxes due to inland water and riverine export were also prepared by McGrath *et al.* (2023) utilizing maps described in Zscheischler *et al.* (2017), and climatological data combined with statistical model and gas transfer velocities.

Data Processing and analysis

### Carbon balances and evaluation of uncertainties

To calculate the country total and biospheric CO$_2$ balances, we retrieved Finland's geographi-

cal area (Fig. 1) from the collection of model output files, each with varying resolutions. The total CO$_2$ balance (sum of biospheric and fossil fuel fluxes) of Finland was determined from both the NGHGI and TD estimates. The TD total balance was estimated based on inversion ensemble that consisted of the newest inversions with the highest resolutions over Finland (CSR, LUMIA, CIF, and CT). The assimilated CO$_2$ net balance obtained from inversion ensemble was computed as a sum of optimized land CO$_2$ fluxes and the prescribed fossil fuel fluxes. Prescribed fossil fuel fluxes of V2021 inversions and CT were derived from inventory data products (see Table 1) that have been distributed in space and time using, e.g., COFFEE approach (McGrath *et al.* 2023, Steinbach *et al.* 2011). The total CO$_2$ balance from TD approaches is given as the median of the ensemble, and uncertainty is denoted with the ensemble min-max range. The total balance obtained from NGHGI was the sum of all UNFCCC emission sectors and their uncertainties.

Similar to the total CO$_2$ balances of Finland, the biospheric CO$_2$ balances from terrestrial ecosystem models and atmospheric inversions were estimated as model ensemble medians, and the uncertainty ranges were illustrated with the spread of the estimates. The spread of estimates provides a range of uncertainty that stems from the structural differences between the models as well as the influence of distinct driver data and parameters used in simulations. The NGHGI uncertainties were taken from EU-level uncertainty analysis that implements procedures to harmonize and gap-fill country-level approach 1 uncertainty estimates (Gaussian error propagation method). The estimated uncertainty for total LULUCF sector in Finland was 65% (McGrath *et al.* 2023).

NBP anomaly – SPEI

With the interest of understanding the interannual variability in ecosystem model and atmospheric inversion results, we computed Pearson correlation coefficients for growing season NBP anomalies and Standardized Precipitation Evapotranspiration Index (SPEI). We used 3-month
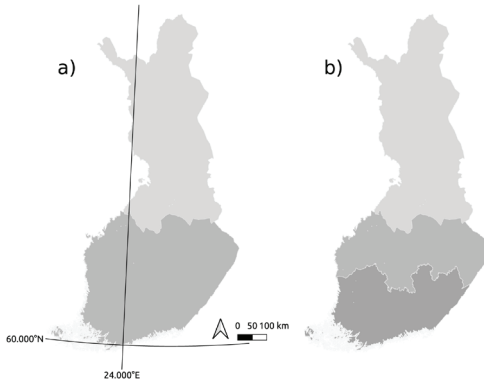
Fig 1. Administrative borders of Finland and the different areas used for analysis. **a)** Northern and southern Finland; **b)** southern, central and northern Finland.

SPEI, and the growing season each year covered June, July, and August. NBP anomaly was computed individually for each simulation using the longest possible time series mean, the time series ranging from 15 years to 31 years. We obtained gridded 3-month SPEI from monthly mean precipitation and temperature data that had been spatially interpolated from observations over the area of Finland on a 10 km X 10 km grid (Aalto *et al.* 2016). The climate data is available at [https://paituli.csc.fi], last accessed: [14th of September 2023] and SPEI was computed according to python code provided by Adams (n.d.). Correlation of SPEI and NBP anomaly spatial mean values were assessed for both the northern and southern Finland (Fig. 1a).

Comparison of spatially explicit forest growth model and atmospheric observations

We evaluated the NEE from the forest growth simulator PREBAS against NBP derived from atmospheric observations by V2021 high-resolution atmospheric inversions. PREBAS solely accounts for CO_2 emissions from forest ecosystems, differing from the inversion's wider scope that includes all fluxes from the terrestrial biosphere (see Terrestrial Ecosystems section). To improve the alignment of these data products, we mapped out Finland's predominantly forested regions using Corine land use data (Corine 2018)

and selected grid cells with varying shares of forest in them (> 0%, > 50%, and > 70% forest cover). The aim was to investigate if exclusion of areas with less forest cover could lead to better alignment between the inversion and PREBAS bottom-up fluxes. To compare different climatological areas, Finland was divided into three sections shown in Fig. 1b.

Gridded inversion fluxes were aggregated to the nine-year averages, covering the years 2012–2020 because the available PREBAS output was the average annual NEE of nine years (2017–2025). The years did not align exactly, however the PREBAS simulation had been run using current climatic conditions, thus the average fluxes were considered to be similar. Inversion NBPs were compared against bottom-up NEEs because that corresponds to the total CO_2 exchange in each grid cell. At the grid cell level, determining the precise location of emissions from harvested wood detected by inversions remains a challenge. This is because the emissions from harvested wood can be emitted at various locations and times after the actual harvest took place. Therefore, NEE is likely to provide a more accurate comparison between the approaches.

Results

Total CO_2 balance of Finland

We estimated Finland's total CO_2 balance from both the NGHGI and optimized CO_2 fluxes from regional high resolution atmospheric inversions (Fig. 2). The spread of estimates in TD ensemble resulted in significantly larger uncertainty range of the total CO_2 balance than suggested by the NGHGI. In addition, the median value of the TD ensemble differed from the NGHGI specifically towards the end of the time series.

The inventory showed a slight increase in the total CO_2 emissions (red in Fig. 2): in 1990, the reported emissions stood at 7.62 Mt C yr^{-1}, while in 2021 the corresponding emissions were 9.77 Mt C yr^{-1}. However, the NGHGI time series did not display a statistically significant trend, given that the annual emissions fluctuated between 3.76 and 11.61 Mt C yr^{-1}. The ensemble
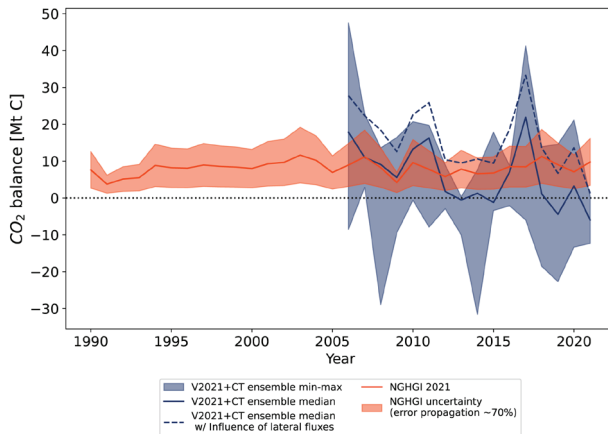
Fig 2. Total CO$_2$ balance of Finland estimated from Finnish national greenhouse gas inventory (NGHGI 2021) and atmospheric inversion ensemble (V2021 + CT). V2021 + CT includes four high-resolution atmospheric inversions CarboScopeRegional, LUMIA, CIF-CHIMERE and CarbonTracker, the first three of which are regional inversions over Europe.

median from V2021+CT inversions indicated a declining trend in Finland's total CO$_2$ balance mainly due to declining anthropogenic emissions, but some of the inversions reported also increments in terrestrial land flux sinks after 2015 (see the next section). Over the last four years of the time series, the TD ensemble median (solid blue line in Fig. 2) consistently falls below the inventory uncertainty range, estimating Finland's total balance of –5.98 Mt C yr^{-1} in 2021 being sink of CO$_2$, while before 2012 the TD median reported higher total balance than the inventory. The TD ensemble estimate is given with large uncertainty and large interannual variability. Despite the trend, the TD ensemble reported both significantly higher and lower annual emissions than the inventory, the difference of TD estimate to the inventory varying from –17 to 13 Mt C yr^{-1}.

For both net emission estimates, the uncertainty mainly consists of land flux/LULUCF uncertainty. The uncertainty of inventory was only about 5% for non-LULUCF sectors and 65% uncertainty for the LULUCF. For the inversion ensemble, the anthropogenic emissions were only dependent on the prescribed fossil fuel fluxes, and there was around 5 Mt C yr^{-1} divergence between anthropogenic emissions reported in the V2021 inversions and CT.

Terrestrial Ecosystems

Comparison of NGHGI LULUCF net carbon stock change to atmospheric inversions (Fig. 3)

and DGVMs (Fig. 4), highlighted the uncertainty related to terrestrial ecosystem carbon balances. All of the estimates were within similar but extremely large uncertainty ranges, however, the NGHGI reported much smaller uncertainty compared with other approaches.

Looking at time series means (Fig. 5), all individual estimates, except CABLE-POP, approximated that the net carbon budget of Finland's terrestrial ecosystems has been a sink during the studied periods. However, it was evident that all atmospheric inversions and DGVMs demonstrated considerable year-to-year variability, which was not reflected in the NGHGI estimate (Figs. 3 and 4). It is worth noting that comparison of the different land flux estimates is challenging due to differences in terminology and carbon flux components included in the approaches. Therefore, the findings should be viewed as a summary of estimates provided by the two approaches on a national scale, and the different methods can represent components of the carbon cycle that both overlap and diverge.

The time series mean values of inversion methods showed some agreement with the LULUCF mean value of the same period (Fig. 5), but the spread of TD estimates varied annually depending on the ensemble of inversions, resolution and observations in use (Fig. 3). The TD estimate that deviated the most from LULUCF was CSR, estimating a mean sink of –23 ± 13 Mt C which was 448% greater than LULUCF time series average (–4.2 ± 3 Mt C) and well outside its uncertainty estimate. The
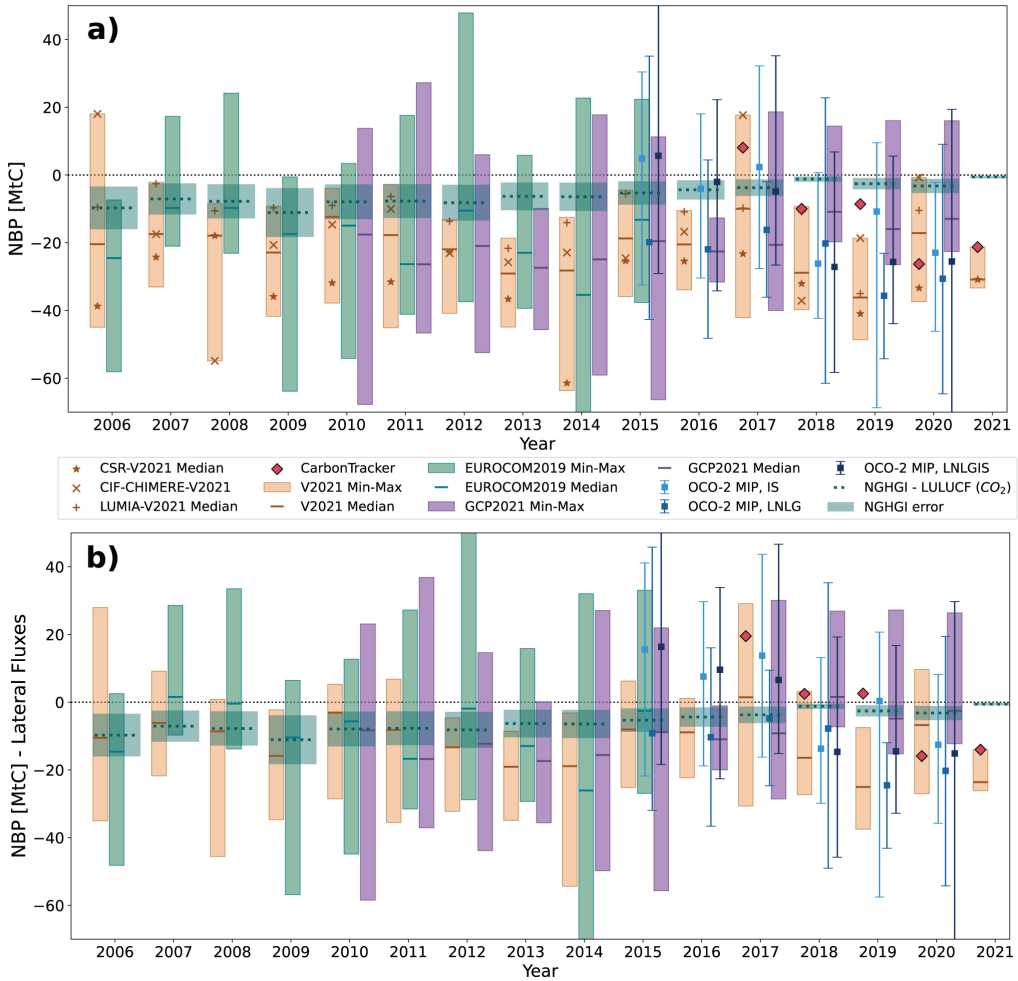
Fig 3. Time series of TD estimates for annual CO_2 land flux balances over Finland. **a**) Original results from the inversions; **b**) inversion results after removing the lateral fluxes. V2021 = ensemble of high-resolution regional inversions from VERIFY 2020 project, EUROCOM2019 = ensemble of six regional inversion from EUROCOM project, GCP2021 = ensemble of global inversions from Global Carbon Project, OCO-2 MIP = ensemble of global inversions from OCO-2 model intercomparison project. IS = assimilated with in-situ measurements, LNLG = assimilated with ACOS v10 land nadir and land glint total column dry-air mole fractions retrieved from OCO-2 satellite, LNLGIS = assimilated with in-situ and satellite observations over land, NGHGI = national greenhouse gas inventory, LULUCF = land use, land use change and forestry sector of NGHGI.
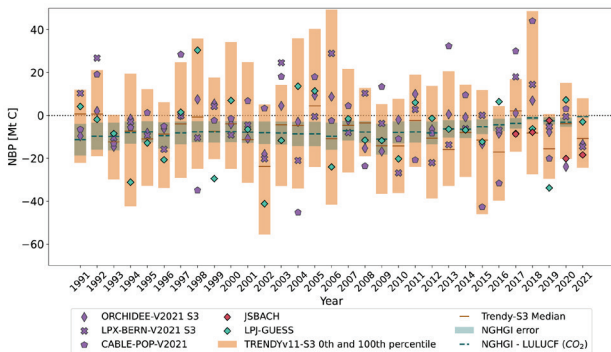
Fig 4. Time series of DGVM estimates for annual biospheric CO_2 balance. TRENDYv11-S3 = ensemble of global DGVM simulations run with standard protocol using time-varying CO_2, climate, and land use forcings. NGHGI LULUCF = national greenhouse gas inventory land use, land use change and forestry sector. Other models, see Table 1.
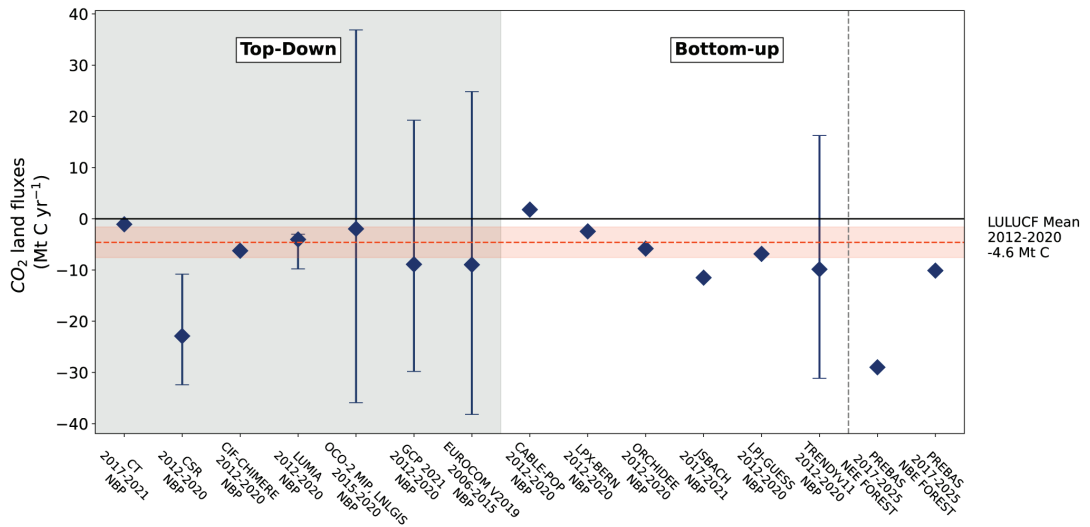
Fig 5. Time series means for top-down and bottom-up estimates. For ensembles the mean estimates are given as the mean of annual ensemble medians, and the error bars represent the mean of annual min and max values. The mean is computed for the nine-year period of 2012–2020 to facilitate comparison with PREBAS results (mean of 2017–2025 with current climate run). If the model/ensemble did not provide results for those years, the closest/longest possible time series mean was computed, e.g. CT simulation covered years 2017–2021. See Table 1 for descriptions of the models/ensembles.

deviation given in the text is the standard deviation of the annual mean values for each estimate whereas in Fig. 5 the error bars represent the annual mean of minimum and maximum values for each ensemble. The other two high-resolution V2021 inversions reported time series mean much closer to the LULUCF, albeit with considerable uncertainty: LUMIA and CIF-CHIMERE estimated a mean sink of -4.0 ± 8.9 Mt C yr^{-1} and -6.2 ± 16 Mt C yr^{-1}, respectively. The lower resolution ensembles EUROCOM, and GCP fell below the LULUCF demonstrating an average sink 110% and 130% greater than the LULUCF. The spread of estimate was highest for the ensembles including higher number of individual atmospheric inversions (GCP, OCO-2 MIP and EUROCOM).

The time series means of CarbonTracker (global inversion) and OCO-2 MIP (global inversion ensemble) aligned closely as both indicated a marginally negative carbon balance (Fig. 5). OCO-2 MIP and CT had the shortest time series available, providing only six and five years of data, respectively. The annual time series (Fig. 3) revealed a consistent pattern between CT and OCO-2 MIP from 2017 to

2020, where both pointed to an increasing trend in the carbon sink capacity of Finnish terrestrial ecosystems which contrasts with LULUCF. That pattern stands out, as the data did not present any other distinguishable trends. Additionally, OCO-2 MIP demonstrated that the selection of atmospheric observations affected the optimized CO₂ fluxes: in-situ measurements (depicted in the lightest blue in Fig. 3) prompted the ensemble to yield more positive NBP values compared with satellite measurements over land (LNLG), apart from the year 2018. The uncertainties in satellite-based estimates are significant.

Figures 3a and 3b illustrate how inclusion of lateral carbon fluxes affected the top-down biospheric carbon balances. When inversion fluxes were adjusted to correspond to the LULUCF carbon stock changes within Finland (Fig. 3b), they aligned more closely with the LULUCF data than the original inversions fluxes in Fig. 3a. The annual lateral transport of carbon varied between -7.2 and -12 Mt C yr^{-1}. When contrasting inversion fluxes with LULUCF estimate, another adjustment would be necessary. LULUCF utilized the managed land proxy, which in Finland covers about 80% of the total area. However, the
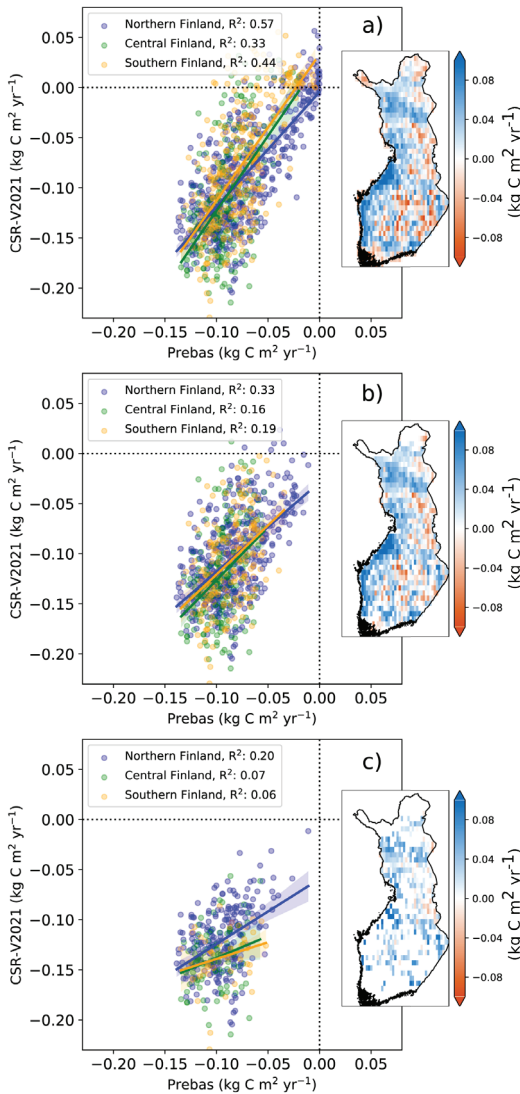
Fig 6. Linear regression between PREBAS and Carbo-ScopeRegional from V2021 model ensemble, including the r^2 values. The estimates are grouped to southern Finland (yellow), central Finland (green) and northern Finland (blue). The maps illustrate the difference between bottom-up and inversion CO_2 fluxes across all grid cells, with red values indicating more positive values (smaller sink) in inversion fluxes. In addition, the maps delineate the spatial distribution of grid cells that satisfied the specified criterion for forest fraction. **a)** Forest fraction > 0; **b)** forest fraction > 0.5; **c)** forest fraction > 0.7.

absence of detailed data on the spatial distribution of managed land complicates the adjustment of inversion fluxes, and consequently that adjustment was excluded from this analysis.

Figure 4 shows the CO_2 fluxes from all DGVMs compared with LULUCF. All simulations had been run using the TRENDY protocol S3 which captures both the direct and indirect anthropogenic emissions/removals from managed and unmanaged land. Comparison of DGVMs and the inventory arose similar results as inversion: the most significant difference between the DGVMs and LULUCF was inter-annual variability reported by DGVMs. In contrast to the inversion estimates, some of the DGVMs (e.g. V2021 simulations) estimated larger than average emissions during the drought years 2006 and 2018. In addition, the TRENDY ensemble demonstrated that the range of estimates derived from DGVMs was comparable to that of the TD approaches. Regardless of the high year-to-year variability, and the large range of estimates, three of the DGVMs mean (Fig. 5) fell within the uncertainty range of LULUCF when comparing the time series mean values. LPX-BERN, ORCHIDEE, LPJ-GUESS were the closest BU estimates approximating an annual sink of –2.5 ± 12 Mt C, –5.8 ± 9.2 Mt C, and –6.9 ± 12 Mt C, respectively.

PREBAS stood out from other BU estimates because it exclusively considered CO_2 fluxes from forest ecosystems, making it not directly comparable to other approaches. However, its NBP was the same order of magnitude as the other estimates at approximately –10 M C yr^{-1}. Its NEE of –29 Mt C yr^{-1} fell close to CSR estimate although conceptually the two differed. PREBAS overestimated the CO_2 sink in forests compared with the LULUCF estimate of the sink capacity on Forest land, which, for a similar 9-year average, was –7 Mt C yr^{-1} (not shown here but can be found in NIR 2023).

Forests

Figure 6 demonstrates that the bottom-up CO_2 fluxes from PREBAS had some congruence with the optimized CO_2 fluxes assimilated in 0.25° × 0.25° resolution by CSR. However, the two lower, 0.5° × 0.5°, resolution inversions displayed a less notable correlation between the approaches (data for lower resolutions shown in Supplements). Additionally, removing grid cells

with low forest fraction typically worsened the regression fit between PREBAS and optimized fluxes.

In this section the optimized fluxes were not adjusted with lateral carbon fluxes, ensuring that they reflected the total CO_2 exchange between the land and atmosphere at each grid cell. The output from PREBAS, which here was the NEE estimate, excluded the anthropogenic disturbances (logging), and thus essentially represented the total CO_2 exchange as well.

Of the high-resolution inversions, CSR had the best fit to PREBAS fluxes, as evidenced by r^2-values ranging from 0.2 and 0.57 in northern Finland. However, fluxes in southern and central Finland demonstrated more divergence. The correlation of the two estimates varied with the number of grid cells included, and consequently the forest fraction. The poorest fits were found when the forest fraction was highest, connected with a relatively low number of grid cells satisfying the criteria (Fig. 6c). Despite the regression showing the poorest fit at a forest fraction of 0.7, the higher forest fraction eliminated most of the fluxes close to zero from both methods which supported the idea that both PREBAS and CSR associated bigger carbon uptake with forested areas.

In terms of differences in flux estimated on grid cell level, and flux distributions across Finland, CSR presented the least biased comparison with PREBAS, indicating both smaller and larger fluxes throughout Finland. However, in specific regions such as Ostrobothnia (Fig. 6a and b) and within the most forested grid cells (Fig. 6c) CSR was more likely to report a larger CO_2 sink compared with PREBAS.

CO_2 fluxes from CSR inversion were also compared against bottom-up forest fluxes from V2021 ORCHIDEE-N model (see Fig. S1 in Supplementary Information). The ORCHIDEE-N output is forest CO_2 flux including the simulation specific disturbances. ORCHIDEE, serving as a prior to one of the CSR runs and for CIF-CHIMERE, revealed that while CSR fitted better with the forest growth model PREBAS, LUMIA and CIF-CHIMERE were more closely aligned with ORCHIDEE. The other two V2021 inversions (see Figs. S2 and S3 in Supplementary Information) were more likely to report

smaller CO_2 sinks across Finland than PREBAS, and the r^2-values were mostly poor. LUMIA demonstrated increasingly negative fluxes moving towards southern Finland, while CIF-CHIMERE displayed a significant dipole pattern in the south of Finland, indicating potential bias in the results.

Interannual variability

The 3-month SPEI drought index explained some of the variability in monthly growing season NBPs according to V2021 DVGMs in southern Finland (Fig 7 a, c, and e). The correlation between 3-month SPEI and monthly NBP anomaly estimated by DVGMs varied from –0.46 to –0.63 suggesting, that during dry growing seasons (negative SPEI values), the southern Finland biosphere might act as a source of CO_2 instead of a sink. In northern Finland, only the CABLE-POP NBP anomaly had statistically significant correlation with SPEI, whereas the other two DVGMs showed no (LPX-Bern 0.05, Fig 3k) or only slight (ORCHIDEE –0.33, Fig. 3g) correlation to SPEI.

The high-resolution regional atmospheric inversions did not display similar correlation to SPEI as DGVMs. Most of the trends between SPEI and inversion carbon balances were not significant (Fig. 7b, d, j, l), and CSR revealed opposite correlation (drought correlated with larger carbon sink) in northern Finland (Fig. 7h). Only CIF-CHIMERE suggested that drought is correlated with higher ecosystem CO_2 emissions in southern Finland (Fig. 7f) with statistically significant correlation coefficient. This correlation (–0.52) was similar to those found in DGVMs.

Discussion

Carbon balances and their uncertainties

The evaluation of Finland's CO_2 budgets showed significant uncertainties primarily stemming from biospheric carbon fluxes (Figs. 2, 3, 4 and 5). A key component of a comprehensive assessment of estimates provided by a range
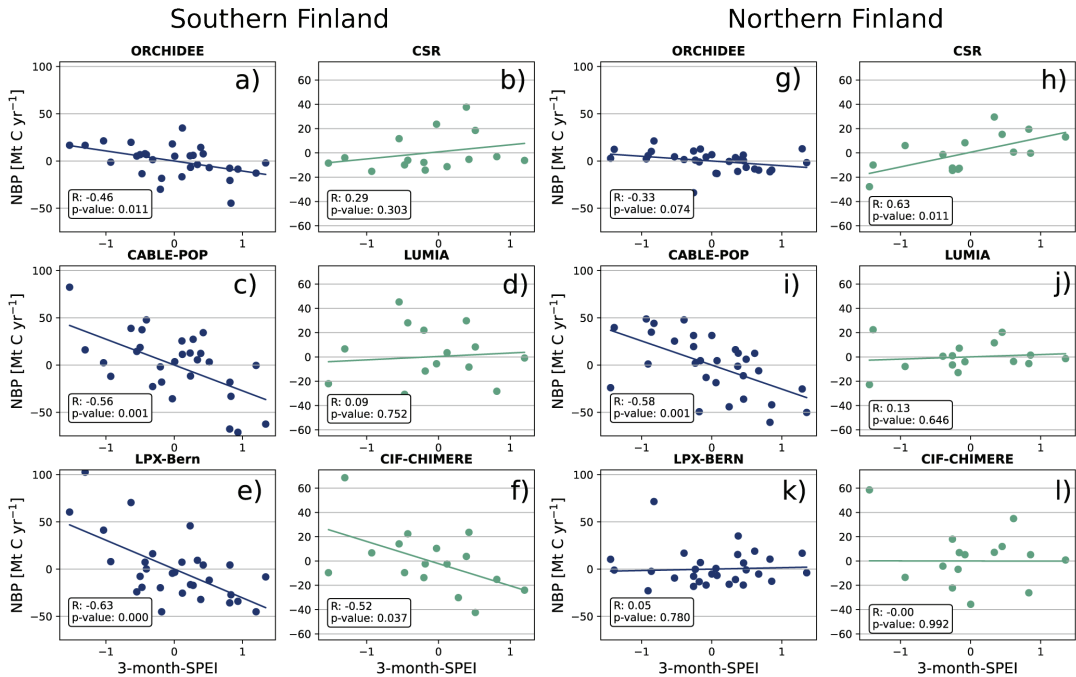
Fig 7. Growing season NBP anomaly of V2021 models as a function of 3-month SPEI. The values of SPEI and NBP anomaly are spatial means. Correlation coefficients (*r*), and their respective statistical significances are given in the box for each pair. **a–f** are representing the mean of southern Finland for both variables and **g–l** are the corresponding values for northern Finland. See Table 1 for descriptions of the models.

of methods involves examining the extent and sources of uncertainty. Here we followed the McGrath *et al.* (2023) quantification of uncertainty: the uncertainties were evaluated from ensembles of simulations, and the TD and BU balances were given as the median of the ensemble. These ensembles were either conducted using multiple models of the same category (DGVMs and inversions; e.g. TRENDY, EURO-COM, OCO-2 MIP) or multiple simulations of a single model (inversions; e.g. CSR, LUMIA). Former category of ensembles can have either harmonized or model-specific inputs whereas the latter ensemble is constructed of simulations of the same model with varying input parameters and forcing data (McGrath *et al.*, 2023). A complete characterization of model uncertainty would require thorough investigation of the spectrum of parameters, input data and model structures (McGrath *et al.*, 2023). However, such an investigation was beyond the scope of this study, given the large number of models involved. Consequently, the uncertainty

presented here provides an insight into the range of estimates and their constraints but does not correspond to the complete description of the uncertainty. The multi-model ensemble proxy is commonly employed by others (Friedlingstein *et al.* 2022, Petrescu *et al.* 2021, 2023) to evaluate the systemic error of TD and BU approaches.

Uncertainty of BU methods have been explored by several authors such as Bastos *et al.* (2020), and with specific focus on DGVMs by e.g. Seiler *et al.*, (2022), and Bonan *et al.* (2019). Uncertainties associated with bottom-up fluxes from DGVMs include: (1) forcing data (Bonan *et al.*, 2019); (2) datasets of land use change and coverage of different land use change practices (Bastos *et al.*, 2022); (3) model parameters; and (4) structural uncertainty resulting from the number of processes included (Petrescu *et al.*, 2021; Houghton *et al.*, 2012). Discrepancy between the terrestrial ecosystem models can also originate from inadequate or inaccurate description of the key processes driving the rate of photosynthesis (Kondo *et al.*, 2020).

Processes that are often poorly modeled or non-existing include forest regrowth, wood harvesting, forest degradation, and aging of the forests, all of which should be reflected to the Finnish NGHGI through the forest inventories. Therefore, regional estimates from global biosphere models should be interpreted with care but can be valuable for understanding the effects of environmental changes on carbon dynamics on both global and regional scales.

Further, the discussion about comparability of DGVMs and inventory carbon balances is still under debate. Both McGrath *et al.* (2023) and Bastos *et al.* (2022) pointed out that it is unclear if the TRENDY protocol S3 (presented here) or the difference between S3 and S2 (see e.g. Friedlingstein *et al.*, 2022) applied to run the DGVM simulations results in a more consistent comparison with anthropogenic emissions/removals captured by NGHGI. Additionally, Grassi *et al.* (2022) has proposed a framework to increase the conceptual comparability between DGVMs and NGHGI which should be considered in the future but was not applied here. Regardless of these concerns, we found the DGVM ensemble (including ORCHIDEE-N, LPX-BERN, CABLE-POP, LPJ-GUESS, JSBACH) agreed closest with the annual mean of NGHGI as the DGVM ensemble reported a mean sink of –4.6 [–21 … +13] Mt C yr^{-1} between years 2012–2020. On the other hand, the other ensemble of DGVMs (TRENDY) suggested a considerably larger sink of –9.9 [–30 … +15] Mt C yr^{-1}, which was outside the LULUCF uncertainty range. Consequently, the number and type of ecosystem-models together with forcing data and resolution utilized in the ensemble influenced the carbon balance estimates.

Uncertainty in posterior inversion fluxes have been found to be large and to differ between countries (Bastos *et al.*, 2022). The main sources of uncertainties in TD approaches are: (1) errors in atmospheric transport models; (2) sparse surface observations and/or incomplete information of the observations causing the inversion flux to be dependent on the prior fluxes; (3) systemic errors in the in-situ and satellite measurements, particularly problematic in regional inversions; and (4) low resolution of the inversion fluxes (McGrath *et al.*, 2023). Inversions included in

this study were the highest resolution inversions published to this date, including a considerable number of in-situ, and satellite observations. The uncertainties of the satellite-based OCO-2 MIP results are the largest of all averaged TD results in Fig. 5. It is worth highlighting that OCO-2 satellite observations are close to the edges of their applicability when using them to estimate fluxes for a small-sized, high-latitude country such as Finland. To reduce the uncertainties that originate from the satellite observations, both the spatial and temporal coverage of the satellite observations should be increased. This is the goal for the next-generation carbon monitoring missions in preparation, most importantly the Copernicus Anthropogenic CO₂ Monitoring (CO2M) mission.

The inversions included both global and regional simulations. The best agreement with LULUCF within TD approaches was found in global TD ensemble (GCP, OCO-2 MIP, CT) that approximated CO₂ sink of –7.3 [-49 +32] Mt C yr^{-1} during the years 2012–2020, while the corresponding values for regional high-resolution inversion ensemble (CSR, CIF, LUMIA) produced an estimate (–12 [–32 +2.8] Mt C yr^{-1}) furthest from the LULUCF. This difference may arise from the small number of regional inversions. One ensemble member (CSR) suggested much larger CO₂ sink in Finland while the other two (LUMIA and CIF) were much closer to the NGHGI and other BU estimates. Individual ensemble members have been found to cause bias especially if the number of ensemble members is low (McGrath *et al.*, 2023). The discrepancy found between inversion estimates may also result from other reasons, e.g., the utilization of sparse and unrepresentative observational data within the complex ecosystem, along with inaccurate meteorological data, emphasizing the need for continuous improvement.

The datasets that are used to post-process the optimized inversion fluxes induce another source of uncertainty to regional inversion balances and the use of inversion estimates to verify NGHGIs (Bastos *et al.*, 2022; Byrne *et al.* 2023). Here, the inversion fluxes were adjusted using lateral flux data product compiled by McGrath *et al.* (2023) based on trade data from FAO

combined with riverine export of carbon. The adjustment of inversion fluxes is done to convert the land-atmosphere CO_2 flux to net carbon stock change which in principle would be equal to NGHGI (Ciais *et al.* 2006). The data product that was used here to achieve comparability between inversion fluxes and NGHGI should be investigated more carefully. Incorporating lateral fluxes enhanced the congruence between LULUCF and inversion fluxes (Fig. 3b), yet it diminished the alignment with the total CO_2 balance when all NGHGI sectors and fossil emissions from inversion were considered (Fig. 2). Consequently, more efforts need to be put on creating national data products that could be used to increase the comparability of inversion and inventory estimates. Using global databases may not yield precise trade data, particularly for smaller countries like Finland. Additionally, relying on national statistics could lead to easier interpretation of inversion results and more confidence to use them to verify national inventories.

We did not consider the fact that LULUCF is conducted with "managed land" proxy, however in the future this is an adjustment that should be made if inventories are verified using other data products. In Finland managed land covers about 80% of the total area leaving 20% of the ecosystems outside whereas DGVMs and atmospheric inversions account for the total area of Finland. However, there is not spatially explicit information of where these managed lands are located making it challenging to accurately consider these in the inversion/DGVM results. Global approximation of the spatial extent of these managed lands has been proposed e.g. by Deng *et al.* (2022), however for national analysis their approach might have led to insufficient assessment in terms of resolution.

Interannual variability

The effect of climatic variability on ecosystem CO_2 uptake has been found in measurements e.g. by Zu *et al.* (2020) and Rinne *et al.* (2020). Extreme droughts and low soil water content can reduce the ecosystem's carbon uptake, potentially turning regional ecosystems carbon neutral or even sources of carbon (e.g., Thompson *et*

al. 2020). Consequently, climate variability can cause fluctuation in the amount of carbon that is absorbed by the biosphere annually, which can be captured by methods that operate on sub-annual time step (Petrescu *et al.* 2021). The effects of climate variability on carbon uptake have been found both in studies utilizing ecosystem models (Piao *et al.* 2013), and atmospheric inversions (Thompson *et al.* 2020, Rödenbeck *et al.* 2020).

The study demonstrated that all individual DGVMs and atmospheric inversions effectively captured year-to-year variations on growing season biospheric fluxes within Finland but only DGVMs could factor in the effect of climatic variables such as temperature and rainfall. Thus, the drivers of this variability remained ambiguous in the inversion methods. He *et al.* (2023) discovered that inversions that assimilated satellite XCO_2 or environmental variables along with in-situ CO_2 observations were more successful at identifying anomalies in biospheric carbon uptake. Potentially owing to limitations in observational data, the three regional inversions we investigated, exclusively assimilating in-situ observations, were unable to capture the effect of extreme drought events on growing season carbon uptake. DGVMs on the other hand, displayed a clear correlation to SPEI, but DGVMs have also been discovered to overemphasize the relationship between NBP and precipitation, as noted by Piao *et al.* (2013). Commonly to inventory methods, only a little of the year-to-year fluctuation was reported in the LULUCF that showed minor reduction in sink capacity over an extreme drought year 2018. Inventories are averaged over multiple years (forest inventory is conducted every five years), and thus they are unable to capture the effects of sub-annual climate variations. However, the ability to account for extreme weather events might have significant relevance to the total biospheric carbon balance in Finland as suggested especially by DGVMs.

Comparison of PREBAS and inversion fluxes

The assessment of regional inversions against forest growth model PREBAS revealed that the

resolution of inversions was too low and the uncertainty too high to make reliable validation of spatially explicit BU fluxes against the observation-based flux estimates. However, PREBAS provided an interesting reference point for comparison due to its high resolution and exact representation of forest structure throughout Finland. Contrasting the gridded inversion fluxes against PREBAS output we found that the spatial distribution of inversion fluxes over Finland were biased specifically for LUMIA, and CIF-CHIMERE. CIF-CHIMERE displayed clear flux "dipole" (Peylin *et al.* 2002) at the capital region of Finland. The dipole effect is a phenomenon where budgets of two neighboring regions are anticorrelated because the sum of that region can be more reliably constrained from large-scale signals (Kondo *et al.* 2020). Dipoles increase the uncertainty in regional inversion fluxes (Kondo *et al.* 2020). LUMIA on the other hand, disclosed a gradient in fluxes between the southern and northern Finland the largest sinks being in southern Finland.

The higher resolution of inversion fluxes appeared to enhance the spatial distribution of these fluxes and reduce biases in comparison to PREBAS, underscoring the benefits of high-resolution inversion results. Moving towards finer spatial resolution of the atmospheric transport models has been on the agenda of inverse modeling community to allow more reliable interpretation of the fluxes and reduce uncertainty in the estimates (e.g. Chevallier 2023). A higher resolution could also facilitate better identification of various land-use types, like forests in this case, potentially leading to easier comparison between different approaches. Now the exclusion of less forested areas diminished the regression fit between CSR and PREBAS, which could be partly due to the extensive spatial averaging applied to PREBAS leading to poor representation of forested areas. The correlation between the CSR and PREBAS was probably partly explained by southern-northern climatic gradient rather than how much forest there was in each grid cell. The regression fit best within the northern Finland which has significant internal climatic gradient resulting in less carbon uptake in the north and more moving towards the south.

Conclusion

This paper investigated the Finnish CO$_2$ balance estimates from broad range of newest research datasets emphasizing the biospheric fluxes. The datasets included both global and regional bottom-up and top-down approaches that were brought to national context for improved understanding of carbon dynamics in Finland, as well as more profound understanding of biospheric balance estimates available and their representativeness in Finland. The newest estimates of biospheric balances within Finland were contrasted against the Finnish national inventory and spatially explicit forest growth model PREBAS that offered precise representation of forest structure throughout Finland. Further, we investigated the relationship between climatic variability and Net Biome Production anomalies from the range of estimates.

In conclusion, this study on Finland's CO$_2$ budgets revealed several important insights into the available estimates of biospheric carbon fluxes. Firstly, the carbon balance estimates from various models and approaches, including DGVMs, satellite or in-situ measurement-based atmospheric inversions, and inventories, were found to be within similar, but large, uncertainty ranges. Secondly, atmospheric inversions generally indicated a larger carbon sink than other methods, but the divergence was reduced when these inversion estimates were adjusted with lateral fluxes, which aligned them more closely with the bottom-up approaches. Thirdly, the study observed interannual variability in carbon flux estimates other than the national inventory. This variability in the inversion models however was not driven by climatic factors, in contrast with the trends observed in DGVMs. This highlights a potential area for further research. Additionally, the benefits of moving towards finer resolution inversion were evident, which is even further supported by the next-generation, high-intensity satellite data.

Furthermore, we want to highlight the importance of collaboration and dialogue between different stakeholders and researchers in the field. By sharing insights and methodologies, there can be a more unified and accurate understanding of carbon dynamics, which is crucial for accurate accounting of regional carbon budgets.

Supplementary Information: The supplementary information related to this article is available online at: http://www.borenv.net/BER/archive/pdfs/ber29/ber29-077-102-supplement.pdf

References

Baldocchi D., Chu H., & Reichstein M. 2018. Inter-annual variability of net and gross ecosystem carbon fluxes: A review. *Agricultural and Forest Meteorolog*y 249: 520–533, https://doi.org/10.1016/j.agrformet.2017.05.015

Bastos A., Ciais P., Sitch S., Aragão L. E. O. C., Chevallier F., Fawcett D., Rosan T. M., Saunois M., Günther D., Perugini L., Robert C., Deng Z., Pongratz J., Ganzenmüller R., Fuchs R., Winkler K., Zaehle S., & Albergel C. 2022. On the use of Earth Observation to support estimates of national greenhouse gas emissions and sinks for the Global stocktake process: Lessons learned from ESA-CCI RECCAP2. *Carbon Balance and Management 17*, 15, https://doi.org/10.1186/s13021-022-00214-w

Bastos A., O'Sullivan M., Ciais P., Makowski D., Sitch S., Friedlingstein P., Chevallier F., Rödenbeck C., Pongratz J., Luijkx I. T., Patra P. K., Peylin P., Canadell J. G., Lauerwald R., Li W., Smith N. E., Peters W., Goll D. S., Jain A. K., Kato E., Lienert S., Lombardozzi D. L., Haverd V., Nabel J. E. M. S., Poulter B., Tian H., Walker A. P., Zaehle, S. 2020. Sources of Uncertainty in Regional and Global Terrestrial CO2 Exchange Estimates. *Global Biogeochemical Cycles 34*(2), e2019GB006393, https://doi.org/10.1029/2019GB006393

Berchet A., Sollum E., Thompson R. L., Pison I., Thanwerdas J., Broquet G., Chevallier F., Aalto T., Bergamaschi P., Brunner D., Engelen R., Fortems-Cheiney A., Gerbig C., Groot Zwaaftink C. D., Haussaire J.-M., Henne S., Houweling S., Karstens U., Kutsch W. L., Luijkx I. T., Monteil G., Palmer P. I., van Peet J. C. A., Peters W., Peylin P., Potier E., Rödenbeck C., Saunois M., Scholze M., Tsuruta A., & Zhao Y. 2021. The Community Inversion Framework v1.0: a unified system for atmospheric inversion studies, *Geosci. Model Dev. 14:* 5331–5354, https://doi.org/10.5194/gmd-14-5331-2021

Bonan G. B., Lombardozzi D. L., Wieder W. R., Oleson K. W., Lawrence D. M., Hoffman F. M., & Collier N. 2019. Model Structure and Climate Data Uncertainty in Historical Simulations of the Terrestrial Carbon Cycle (1850–2014). *Global Biogeochemical Cycles 33*(10): 1310–1326, https://doi.org/10.1029/2019GB006175

Broquet G., Chevallier F., Bréon F.-M., Kadygrov N., Alemanno M., Apadula F., Hammer S., Haszpra L., Meinhardt F., Morguí J. A., Necki J., Piacentino S., Ramonet M., Schmidt M., Thompson R. L., Vermeulen A. T., Yver C., & Ciais P. 2013. Regional inversion of CO2 ecosystem fluxes from atmospheric measurements: Reliability of the uncertainty estimates. *Atmospheric Chemistry and Physics 13:* 9039–9056, https://doi.org/10.5194/acp-13-9039-2013

Byrne B., Baker D. F., Basu S., Bertolacci M., Bowman K. W., Carroll D., Chatterjee A., Chevallier F., Ciais P., Cressie N., Crisp D., Crowell S., Deng F., Deng Z., Deutscher N. M., Dubey M. K., Feng S., García O. E., Griffith D. W. T., Herkommer B., Hu L., Jacobson A. R., Janardanan R., Jeong S., Johnson M. S., Jones D. B. A., Kivi R., Liu J., Liu Z., Maksyutov S., Miller J. B., Miller S. M., Morino I., Notholt J., Oda T., O'Dell C. W., Oh Y.-S., Ohyama H., Patra P. K., Peiro H., Petri C., Philip S., Pollard D. F., Poulter B., Remaud M., Schuh A., Sha M. K., Shiomi K., Strong K., Sweeney C., Té Y., Tian H., Velazco V. A., Vrekoussis M., Warneke T., Worden J. R., Wunch D., Yao Y., Yun J., Zammit-Mangion A., & Zeng N. 2023. National CO2 budgets (2015–2020) inferred from atmospheric CO2 observations in support of the global stocktake. *Earth Syst. Sci. Data 15:* 963–1004, https://doi.org/10.5194/essd-15-963-2023

Chevallier F., Lloret Z., Cozic A., Takache S., & Remaud M. 2023. Toward High-Resolution Global Atmospheric Inverse Modeling Using Graphics Accelerators. *Geophysical Research Letters 50,* e2022GL102135, https://doi.org/10.1029/2022GL102135

Chevallier F. 2021. Fluxes of carbon dioxide from managed ecosystems estimated by national inventories compared to atmospheric inverse modeling. *Geophysical Research Letters*, 48, e2021GL093565, https://doi.org/10.1029/2021GL093565

Ciais P., Bastos A., Chevallier F., Lauerwald R., Poulter B., Canadell J. G., Hugelius G., Jackson R. B., Jain A., Jones M., Kondo M., Luijkx I. T., Patra P. K., Peters W., Pongratz J., Petrescu A. M. R., Piao S., Qiu C., Von Randow C., Regnier P., Saunois M., Scholes R., Shvidenko A., Tian H., Yang H., Wang X. & Zheng B. 2022. Definitions and methods to estimate regional land carbon fluxes for the second phase of the REgional Carbon Cycle Assessment and Processes Project (RECCAP-2). *Geosci. Model Dev. 15:* 1289–1316, https://doi.org/10.5194/gmd-15-1289-2022

Ciais P., Borges A. V., Abril G., Meybeck M., Folberth G., Hauglustaine D., and Janssens I. A. 2008. The impact of lateral carbon fluxes on the European carbon balance.

Biogeosciences 5: 1259–1271, https://doi.org/10.5194/bg-5-1259-2008

Corine. 2018. CORINE Land Cover 2018 dataset. Available at: [https://www.avoindata.fi/data/fi/dataset/corine-maanpeite-2018]. last accessed: [4.8.2023].

CRF. 2023. Finland's 2023 Common Reporting Format (CRF) Table. Available: [https://unfccc.int/documents/627719] Last accessed: [17. November 2023].

Crisp D., Dolman H., Tanhua T., McKinley G. A., Hauck J., Bastos A., Sitch S., Eggleston S., & Aich V. 2022. How Well Do We Understand the Land-Ocean-Atmosphere Carbon Cycle? *Reviews of Geophysics 60*, e2021RG000736, https://doi.org/10.1029/2021RG000736

Deng Z., Ciais P., Tzompa-Sosa Z. A., Saunois M., Qiu C., Tan C., Sun T., Ke P., Cui Y., Tanaka K., Lin X., Thompson R. L., Tian H., Yao Y., Huang Y., Lauerwald R., Jain A. K., Xu X., Bastos A., Sitch S., Palmer P. I., Lauvaux T., d'Aspremont A., Giron C., Benoit A., Poulter B., Chang J., Petrescu A. M. R., Davis S. J., Liu Z., Grassi G., Albergel C., Tubiello F. N., Perugini L., Peters W. & Chevallier F. 2022. Comparing national greenhouse gas budgets reported in UNFCCC inventories against atmospheric inversions. *Earth Syst. Sci. Data 14:* 1639–1675, https://doi.org/10.5194/essd-14-1639-2022

Ducoudré N. I., Laval K., & Perrier A. 1993. SECHIBA, a New Set of Parameterizations of the Hydrologic Exchanges at the Land-Atmosphere Interface within the LMD Atmospheric General Circulation Model. *Journal of Climate 6:* 248–273, http://www.jstor.org/stable/26197219

EU. 2021. Regulation (EU) 2021/1119 of the European Parliament and of the Council of 30 June 2021 establishing the framework for achieving climate neutrality and amending Regulations (EC) No 401/2009 and (EU) 2018/1999 ("European Climate Law"), Available: [https://eur-lex.europa.eu/legal-content/EN/TXT/?uri=CELEX:32021R1119]. Last accessed: [12. November 2023]

Finnish Government. 2022. Climate Law (423/2022). Available at: [https://www.finlex.fi/fi/laki/ajantasa/2022/20220423?search%5Btype%5D=pika&search%5Bpika%5D=ilmastolaki]. Last accessed: [12.11.2023].

Forsius M., Holmberg M., Junttila V., Kujala H., Schulz T., Paunu V.-V., Savolahti M., Minunno F., Akujärvi A., Bäck J., Grönroos J., Heikkinen R. K., Karvosenoja N., Mäkelä A., Mikkonen N., Pekkonen M., Rankinen K. & Virkkala R. 2023. Modelling the regional potential for reaching carbon neutrality in Finland: Sustainable forestry, energy use and biodiversity protection. *Ambio 52:* 1757–1776, https://doi.org/10.1007/s13280-023-01860-1

Fortems-Cheiney A., Pison I., Broquet G., Dufour G., Berchet A., Potier E., Coman A., Siour G. & Costantino L. 2021. Variational regional inverse modeling of reactive species emissions with PYVAR-CHIMERE-v2019. *Geosci. Model Dev. 14:* 2939–2957, https://doi.org/10.5194/gmd-14-2939-2021

Friedlingstein P., O'Sullivan M., Jones M. W., Andrew R. M., Gregor L., Hauck J., Le Quéré C., Luijkx I. T., Olsen A., Peters G. P., Peters W., Pongratz J., Schwingshackl C., Sitch S., Canadell J. G., Ciais P., Jackson R. B., Alin S. R., Alkama R., Arneth A., Arora V. K., Bates N. R., Becker M., Bellouin N., Bittig H. C., Bopp L., Chevallier F., Chini L. P., Cronin M., Evans W., Falk S., Feely R. A., Gasser T., Gehlen M., Gkritzalis T., Gloege L., Grassi G., Gruber N., Gürses Ö., Harris I., Hefner M., Houghton R. A., Hurtt G. C., Iida Y., Ilyina T., Jain A. K., Jersild A., Kadono K., Kato E., Kennedy D., Klein Goldewijk K., Knauer J., Korsbakken J. I., Landschützer P., Lefèvre N., Lindsay K., Liu J., Liu Z., Marland G., Mayot N., McGrath M. J., Metzl N., Monacci N. M., Munro D. R., Nakaoka S.-I., Niwa Y., O'Brien K., Ono T., Palmer P. I., Pan N., Pierrot D., Pocock K., Poulter B., Resplandy L., Robertson E., Rödenbeck C., Rodriguez C., Rosan T. M., Schwinger J., Séférian R., Shutler J. D., Skjelvan I., Steinhoff T., Sun Q., Sutton A. J., Sweeney C., Takao S., Tanhua T., Tans P. P., Tian X., Tian H., Tilbrook B., Tsujino H., Tubiello F., van der Werf G. R., Walker A. P., Wanninkhof R., Whitehead C., Willstrand Wranne A., Wright R., Yuan W., Yue C., Yue X., Zaehle S., Zeng J. & Zheng B. 2022. Global Carbon Budget 2022. *Earth Syst. Sci. Data 14:* 4811–4900, https://doi.org/10.5194/essd-14-4811-2022

Grassi G., House J., Kurz W. A., Cescatti A., Houghton R. A., Peters G. P., Sanz M. J., Viñas R. A., Alkama R., Arneth A., Bondeau A., Dentener F., Fader M., Federici S., Friedlingstein P., Jain A. K., Kato E., Koven C. D., Lee D., Nabel J., Nassikas A., Perugini L., Rossi S., Sitch S., Viovy N., Wiltshire A. & Zaehle, S. 2018. Reconciling global-model estimates and country reporting of anthropogenic forest CO2 sinks. *Nature Climate Change 8:* 914–920, https://doi.org/10.1038/s41558-018-0283-x

Grassi G., Schwingshackl C., Gasser T., Houghton R. A., Sitch S., Canadell J. G., Cescatti A., Ciais P., Federici S., Friedlingstein P., Kurz W. A., Sanz Sanchez M. J., Abad Viñas R., Alkama R., Bultan S., Ceccherini G., Falk S., Kato E., Kennedy D., Knauer J., Korosuo A., Melo J., McGrath M. J., Nabel J. E. M. S., Poulter B., Romanovskaya A. A., Rossi S., Tian H., Walker A. P., Yuan W., Yue X. & Pongratz J. 2023. Harmonising the land-use flux estimates of global models and national inventories for 2000–2020. *Earth Syst. Sci. Data 15:* 1093–1114, https://doi.org/10.5194/essd-15-1093-2023

Haakana M., Haikarainen S., Henttonen H., Hirvelä H., Hynynen J., Korhonen K., Launiainen S., Mehtätalo L., Miettinen A., Mutanen A., Mäkinen H., Ollila P., Pitkänen J., Räty M., Salminen O.-P., Tikkasalo O.-P., Tuomainen T., Viitanen J., Vikfors S. 2022. Suomen LULUCF-sektorin 2021–2025 velvoitteen toteutuminen. Luonnonvarakeskus. http://urn.fi/URN:NBN:-fi-fe2022123074123

Haverd V., Smith B., Nieradzik L., Briggs P. R., Woodgate W., Trudinger C. M., Canadell J. G. & Cuntz M. 2018. A new version of the CABLE land surface model (Subversion revision r4601) incorporating land use and land cover change, woody vegetation demography, and a novel optimisation-based approach to plant coordination

of photosynthesis. *Geosci. Model Dev. 11:* 2995–3026, https://doi.org/10.5194/gmd-11-2995-2018

He W., Jiang F., Ju W., Byrne B., Xiao J., Nguyen N. T., Wu M., Wang S., Wang J., Rödenbeck C., Li X., Scholze M., Monteil G., Wang H., Zhou Y., He Q. & Chen J. M. 2023. Do state-of-the-art atmospheric CO2 inverse models capture drought impacts on the European land carbon uptake? *Journal of Advances in Modeling Earth Systems* 15: e2022MS003150, https://doi.org/10.1029/2022MS003150

IPCC. 2006. *Guidelines for National Greenhouse Gas Inventories, Prepared by the National Greenhouse Gas Inventories Programme*. IGES. Retrieved November 27, 2023, from https://www.ipcc-nggip.iges.or.jp/public/2006gl/

IPCC. 2021. Summary for Policymakers. In Climate Change 2021 – The Physical Science Basis: Working Group I Contribution to the Sixth Assessment Report of the Intergovernmental Panel on Climate Change pp. 3–32. frontmatter, Cambridge: Cambridge University Press. https://doi.org/10.1017/9781009157896.001.

Junttila V., Minunno F., Peltoniemi M., Forsius M., Akujärvi A., Ojanen P. & Mäkelä A. 2023. Quantification of forest carbon flux and stock uncertainties under climate change and their use in regionally explicit decision making: Case study in Finland. *Ambio 52:* 1716–1733, https://doi.org/10.1007/s13280-023-01906-4

Kalliokoski T., Mäkelä A., Fronzek S., Minunno F. & Peltoniemi M. 2018. Decomposing sources of uncertainty in climate change projections of boreal forest primary production. *Agricultural and Forest Meteorology 262:* 192–205, https://doi.org/10.1016/j.agrformet.2018.06.030

Kondo M., Patra P. K., Sitch S., Friedlingstein P., Poulter B., Chevallier F., Ciais P., Canadell J. G., Bastos A., Lauerwald R., Calle L., Ichii K., Anthoni P., Arneth A., Haverd V., Jain A. K., Kato E., Kautz M., Law R. M., Lienert S., Lombardozzi D., Maki T., Nakamura T., Peylin P., Rödenbeck C., Zhuravlev R., Saeki T., Tian H., Zhu D., Ziehn, T. 2020. State of the science in reconciling top-down and bottom-up approaches for terrestrial CO2 budget. *Global Change Biology 26:* 1068–1084, https://doi.org/10.1111/gcb.14917

Korhonen K. T., Ahola A., Heikkinen J., Henttonen H. M., Hotanen J. P., Ihalainen A., Melin M., Pitkänen J., Räty M., Sirviö M. & Strandström M. 2021. Forests of Finland 2014–2018 and their development 1921–2018. *Silva Fennica 55,* https://doi.org/10.14214/sf.10662

Kountouris P., Gerbig C., Rödenbeck C., Karstens U., Koch T. F. & Heimann, M. 2018. Atmospheric CO2 inversions on the mesoscale using data-driven prior uncertainties: quantification of the European terrestrial CO2 fluxes. *Atmos. Chem. Phys. 18:* 3047–3064, https://doi.org/10.5194/acp-18-3047-2018

Krinner G., Viovy N., De Noblet-Ducoudré N., Ogée J., Polcher J., Friedlingstein P., Ciais P., Sitch S. & Prentice I. C. 2005. A dynamic global vegetation model for studies of the coupled atmosphere-biosphere system. *Global Biogeochemical Cycles 19,* 2003GB002199, https://doi.org/10.1029/2003GB002199

Kyoto Protocol to the United Nations Framework Convention on Climate Change, Dec. 10, 1997, 2303 U.N.T.S. 162

Lienert, S. & Joos, F. 2018. A Bayesian ensemble data assimilation to constrain model parameters and land-use carbon emissions, *Biogeosciences 15.* 2909–2930, https://doi.org/10.5194/bg-15-2909-2018

Liski J., Palosuo T., Peltoniemi M. & Sievänen R. 2005. Carbon and decomposition model Yasso for forest soils. *Ecological modelling 189:* 168-182, https://doi.org/10.1016/j.ecolmodel.2005.03.005

Mäkelä A., Minunno F., Kujala H., Kosenius A.-K., Heikkinen R. K., Junttila V., Peltoniemi M. & Forsius M. 2023. Effect of forest management choices on carbon sequestration and biodiversity at national scale. *Ambio 52:* 1737–1756, https://doi.org/10.1007/s13280-023-01899-0

Minunno F., Peltoniemi M., Härkönen S., Kalliokoski T., Makinen H. & Mäkelä A. 2019. Bayesian calibration of a carbon balance model PREBAS using data from permanent growth experiments and national forest inventory. *Forest Ecology and Management 440:* 208–257. https://doi.org/10.1016/j.foreco.2019.02.041

Minunno F., Peltoniemi M., Launiainen S., Aurela M., Lindroth A., Lohila A., Mammarella I., Minkkinen K. & Mäkelä A. 2016. Calibration and validation of a semi-empirical flux ecosystem model for coniferous forests in the Boreal region. *Ecological Modelling 341:* 37–52, https://doi.org/10.1016/j.ecolmodel.2016.09.020

Monteil G., Broquet G., Scholze M., Lang M., Karstens U., Gerbig C., Koch F.-T., Smith N. E., Thompson R. L., Luijkx I. T., White E., Meesters A., Ciais P., Ganesan A. L., Manning A., Mischurow M., Peters W., Peylin P., Tarniewicz J., Rigby M., Rödenbeck C., Vermeulen A. & Walton, E. M. 2020. The regional European atmospheric transport inversion comparison, EUROCOM: first results on European-wide terrestrial carbon fluxes for the period 2006–2015. *Atmos. Chem. Phys. 20:* 12063–12091, https://doi.org/10.5194/acp-20-12063-2020

Monteil G. & Scholze M. 2021. Regional CO2 inversions with LUMIA, the Lund University Modular Inversion Algorithm, v1.0. *Geosci. Model Dev. 14:* 3383–3406, https://doi.org/10.5194/gmd-14-3383-2021

Munassar S., Monteil G., Scholze M., Karstens U., Rödenbeck C., Koch F.-T., Totsche K. U. & Gerbig C. 2023. Why do inverse models disagree? A case study with two European CO2 inversions. *Atmos. Chem. Phys. 23:* 2813–2828, https://doi.org/10.5194/acp-23-2813-2023

Munassar S., Rödenbeck C., Koch F.-T., Totsche K. U., Gałkowski M., Walther S., and Gerbig C. 2022. Net ecosystem exchange (NEE) estimates 2006–2019 over Europe from a pre-operational ensemble-inversion system. *Atmos. Chem. Phys. 22:* 7875–7892, https://doi.org/10.5194/acp-22-7875-2022

NIR. 2023. Finland's 2023 National Inventory Report (NIR). Available: [https://unfccc.int/documents/627718] last accessed: [17. November 2023]

Paris Agreement to the United Nations Framework Convention on Climate Change, Dec. 12, 2015, T.I.A.S. No. 16-1104

Peltoniemi M., Markkanen T., Härkönen S., Thum T., Aalto T. & Mäkelä, A. 2015. Consistent estimates of gross primary production of Finnish forests—Comparison of estimates of two process models. *Luonnonvarakeskus 20*, http://urn.fi/URN:NBN:fi-fe2016082623063

Petrescu A. M. R., Qiu C., McGrath M. J., Peylin P., Peters G. P., Ciais P., Thompson R. L., Tsuruta A., Brunner D., Kuhnert M., Matthews B., Palmer P. I., Tarasova O., Regnier P., Lauerwald R., Bastviken D., Höglund-Isaksson L., Winiwarter W., Etiope G., Aalto T., Balsamo G., Bastrikov V., Berchet A., Brockmann P., Ciotoli G., Conchedda G., Crippa M., Dentener F., Groot Zwaaftink C. D., Guizzardi D., Günther D., Haussaire J.-M., Houweling S., Janssens-Maenhout G., Kouyate M., Leip A., Leppänen A., Lugato E., Maisonnier M., Manning A. J., Markkanen T., McNorton J., Muntean M., Oreggioni G. D., Patra P. K., Perugini L., Pison I., Raivonen M. T., Saunois M., Segers A. J., Smith P., Solazzo E., Tian H., Tubiello F. N., Vesala T., van der Werf G. R., Wilson C. & Zaehle S. 2023. The consolidated European synthesis of CH4 and N2O emissions for the European Union and United Kingdom: 1990–2019. *Earth Syst. Sci. Data 15:* 1197–1268, https://doi.org/10.5194/essd-15-1197-2023

Petrescu A. M. R., McGrath M. J., Andrew R. M., Peylin P., Peters G. P., Ciais P., Broquet G., Tubiello F. N., Gerbig C., Pongratz J., Janssens-Maenhout G., Grassi G., Nabuurs G.-J., Regnier P., Lauerwald R., Kuhnert M., Balkovič J., Schelhaas M.-J., Denier van der Gon H. A. C., Solazzo E., Qiu C., Pilli R., Konovalov I. B., Houghton R. A., Günther D., Perugini L., Crippa M., Ganzenmüller R., Luijkx I. T., Smith P., Munassar S., Thompson R. L., Conchedda G., Monteil G., Scholze M., Karstens U., Brockmann P. & Dolman A. J. 2021. The consolidated European synthesis of CO2 emissions and removals for the European Union and United Kingdom: 1990–2018. *Earth Syst. Sci. Data 13:* 2363–2406, https://doi.org/10.5194/essd-13-2363-2021

Peylin P., Baker D., Sarmiento J., Ciais P. & Bousquet P. 2002. Influence of transport uncertainty on annual mean and seasonal inversions of atmospheric CO2 data. *J. Geophys. Res.* 107: 4385, doi:10.1029/2001JD000857

Piao, S., Sitch, S., Ciais, P., Friedlingstein, P., Peylin, P., Wang, X., Ahlström, A., Anav, A., Canadell, J. G., Cong, N., Huntingford, C., Jung, M., Levis, S., Levy, P. E., Li, J., Lin, X., Lomas, M. R., Lu, M., Luo, Y., Ma Y., Myneni R., Poulter B., Sun Z., Wang T., Viovy N., Zaehle S. & Zeng, N. 2013. Evaluation of terrestrial carbon cycle models for their response to climate variability and to CO2 trends. *Global Change Biology 19:* 2117–2132, https://doi.org/10.1111/gcb.12187

Polcher J., McAvaney B., Viterbo P., Gaertner M.-A., Hahmann A., Mahfouf J.-F., Noilhan J., Phillips T., Pitman A., Schlosser C. A., Schulz J.-P., Timbal B., Verseghy D. & Xue Y. 1998. A proposal for a general interface between land surface schemes and general circulation models. *Global and Planetary Change 19:* 261–276, https://doi.org/10.1016/S0921-8181(98)00052-6

Reick C. H., Gayler V., Goll D., Hagemann S., Heidkamp M., Nabel J. E. M. S., Raddatz T., Roeckner E., Schnur R. & Wilkenskjeld S. 2021. *JSBACH 3 - The land com-*

ponent of the MPI Earth System Model: Documentation of version 3.2 [Application/pdf], 4990986, https://doi.org/10.17617/2.3279802

Rinne J., Tuovinen J.-P., Klemedtsson L., Aurela M., Holst J., Lohila A., Weslien P., Vestin P., Łakomiec P., Peichl M., Tuittila E.-S., Heiskanen L., Laurila T., Li X., Alekseychik P., Mammarella I., Ström L., Crill P. & Nilsson M. B. 2020. Effect of the 2018 European drought on methane and carbon dioxide exchange of northern mire ecosystems. *Philosophical Transactions of the Royal Society B: Biological Sciences 375:* 20190517, https://doi.org/10.1098/rstb.2019.0517

Rödenbeck C., Zaehle S., Keeling R. & Heimann M. 2020. The European carbon cycle response to heat and drought as seen from atmospheric CO2 data for 1999–2018. *Philosophical Transactions of the Royal Society B: Biological Sciences 375:* 20190506, https://doi.org/10.1098/rstb.2019.0506

Seiler C., Melton J. R., Arora V. K., Sitch S., Friedlingstein P., Anthoni P., Goll D., Jain A. K., Joetzjer E., Lienert S., Lombardozzi D., Luyssaert S., Nabel J. E. M. S., Tian H., Vuichard N., Walker A. P., Yuan W., & Zaehle S. 2022. Are Terrestrial Biosphere Models Fit for Simulating the Global Land Carbon Sink? *Journal of Advances in Modeling Earth Systems 14:* e2021MS002946, https://doi.org/10.1029/2021MS002946

Smith B., Prentice I. C. & Sykes M. T. 2001. Representation of Vegetation Dynamics in the Modelling of Terrestrial Ecosystems: Comparing Two Contrasting Approaches within European Climate Space. *Global Ecology and Biogeography 10:* 621–637, http://www.jstor.org/stable/3182691

Smith B., Wårlind D., Arneth A., Hickler T., Leadley P., Siltberg J. & Zaehle, S. 2014. Implications of incorporating N cycling and N limitations on primary production in an individual-based dynamic vegetation model. *Biogeosciences 11:* 2027–2054, https://doi.org/10.5194/bg-11-2027-2014

Steinbach J., Gerbig C., Rödenbeck C., Karstens U., Minejima C. & Mukai H. 2011. The CO2 release and Oxygen uptake from Fossil Fuel Emission Estimate (COFFEE) dataset: effects from varying oxidative ratios. *Atmos. Chem. Phys. 11:* 6855–6870, https://doi.org/10.5194/acp-11-6855-2011

Tenkanen M. K., Tsuruta A., Tyystjärvi V., Törmä M., Autio I., Haakana M., Tuomainen T., Leppänen A., Markkanen T., Raivonen M., Niinistö S., Nadir Arsian A. & Aalto T. 2023. Using Atmospheric Inverse Modelling of Methane Budgets with Copernicus Land Water and Wetness Data to Detect Land Use-Related Emissions. *Remote Sensing 16:* 124, https://doi.org/10.3390/rs16010124

Thompson R. L., Broquet G., Gerbig C., Koch T., Lang M., Monteil G., Munassar S., Nickless A., Scholze M., Ramonet M., Karstens U., Van Schaik E., Wu Z. & Rödenbeck C. 2020. Changes in net ecosystem exchange over Europe during the 2018 drought based on atmospheric observations. *Philosophical Transactions of the Royal Society B: Biological Sciences 375:* 20190512, https://doi.org/10.1098/rstb.2019.0512

Tonteri T., Hotanen J.-P., Mäkipää R., Nousiainen H., Reini-

kainen A. & Tamminen M. 2005. Metsäkasvit kasvupai-
koillaan—kasvupaikkatyypin, kasvillisuusvyöhykkeen,
puuston kehitysluokan ja puulajin yhteys kasvilajien
runsaussuhteisiin. *Metsäntutkimuslaitoksen Tiedonan-
toja 946, http://urn.fi/URN:ISBN:951-40-1982-2*

Valentine H. T. & Mäkelä A. 2005. Bridging process-ba-
sed and empirical approaches to modeling tree growth.
Tree Physiology 25: 769–779, https://doi.org/10.1093/
treephys/25.7.769

Van Der Laan-Luijkx, I. T., Van Der Velde, I. R., Van Der
Veen, E., Tsuruta, A., Stanislawska, K., Babenhaus-
erheide, A., Zhang, H. F., Liu, Y., He, W., Chen, H.,
Masarie, K. A., Krol, M. C., & Peters, W. (2017). The
CarbonTracker Data Assimilation Shell (CTDAS) v1.0:
Implementation and global carbon balance 2001–2015.
Geoscientific Model Development, *10*(7), 2785–2800.
https://doi.org/10.5194/gmd-10-2785-2017

van der Laan-Luijkx I. T., van der Velde I. R., van der Veen
E., Tsuruta A., Stanislawska K., Babenhauserheide A.,
Zhang H. F., Liu Y., He W., Chen H., Masarie K. A.,
Krol M. C., and Peters W. 2017. The CarbonTracker
Data Assimilation Shell (CTDAS) v1.0: implementation
and global carbon balance 2001–2015. *Geosci. Model
Dev. 10:* 2785–2800, https://doi.org/10.5194/gmd-10-
2785-2017

Viovy N. 1996. Interannuality and CO2 sensitivity of the
SECHIBA-BGC coupled SVAT-BGC model. *Physics
and Chemistry of the Earth 21:* 489-497, https://doi.

org/10.1016/S0079-1946(97)81147-0

Woodward F. I. & Cramer W. 1996. Plant functional
types and climatic change: Introduction. *Jour-
nal of Vegetation Science 7:* 306–308, https://doi.
org/10.1111/j.1654-1103.1996.tb00489.x

Zscheischler J., Mahecha M. D., Avitabile V., Calle L.,
Carvalhais N., Ciais P., Gans F., Gruber N., Hartmann
J., Herold M., Ichii K., Jung M., Landschützer P.,
Laruelle G. G., Lauerwald R., Papale D., Peylin P.,
Poulter B., Ray D., Regnier P., Rödenbeck C., Roman-
Cuesta R. M., Schwalm C., Tramontana G., Tyukavina
A., Valentini R., van der Werf G., West T. O., Wolf J.
E. & Reichstein M. 2017. Reviews and syntheses: An
empirical spatiotemporal description of the global sur-
face–atmosphere carbon fluxes: opportunities and data
limitations. *Biogeosciences 14.* 3685–3703, https://doi.
org/10.5194/bg-14-3685-2017

Fu Z., Ciais P., Bastos A., Stoy P. C., Yang H., Green J.
K., Wang B., Yu K., Huang Y., Knohl A., Šigut L.,
Gharun M., Cuntz M., Arriga N., Roland M., Peichl M.,
Migliavacca M., Cremonese E., Varlagin A., Brümmer
C., Gourlez de la Motte L., Fares S., Buchmann N.,
El-Madany T., Pitacco A., Vendrame N., Li Z., Vincke
C., Magliulo E. & Koebsch, F. 2020. Sensitivity of
gross primary productivity to climatic drivers during
the summer drought of 2018 in Europe. *Philosophical
Transactions of the Royal Society B: Biological Sciences
375:* 20190747, https://doi.org/10.1098/rstb.2019.0747